[5]李霞,杨静,麻军,等. 乌鲁木齐重污染日的天气分型和边界层结构特征研究[J]. 高原气象,2012,31(5)：1414~1423.

[6]赵克明,李霞,杨静. 乌鲁木齐最大混合层厚度变化的环境响应[J]. 干旱区研究,2011,28(3)：509~513.

[7]杨静，武疆艳，李霞. 乌鲁木齐冬季大气边界层结构特征及其对大气污染的影响[J]. 干旱区研究，2011，28(4)：718~723.

[8]杨静，李霞，李琴.乌鲁木齐近30年大气稳定度和混合层高度变化特征及其对空气污染的影响[J]. 干旱区地理，2011，28(3)：747~752.

[9]李景林,郑玉萍,刘增强.乌鲁木齐市低空温度层结与采暖期大气污染的关系[J].干旱区地理,2007,30(4)：519~525.

[10]李东方.乌鲁木齐市环境空气中主要污染物24h变化特征[J].干旱环境监测,2003,17(4):233~235.

[11]钱翌,巴雅尔塔.乌鲁木齐市大气污染物时空分布特制研究[J].新疆农业大学学报,2004,27(4):51~55.

[12]魏毅,孟亮,李朝阳. 2004~2010年乌鲁木齐市可吸入颗粒物污染特征[J]. 气象与环境学报,2012，28(1)：82~85.

[13]李新琪，海热提·涂尔逊。乌鲁木齐市大气环境容载力及污染防治对策研究[J]. 干旱区资源与环境，2001，15(3)：17～24。

[14]The Urban air pollution database, by country and city (corrected version). http://www.who.int/phe/health_topics/outdoorair/databases/en/index.html.

[15]王晓雯,王锋,刘鹏等.乌鲁木齐市儿科7年住院病例分析[J].实用临床医学,2005,6(5)：115~117.

[16]李明霞,郭艳芳,朱艳萍. 乌鲁木齐市维、汉族孕妇及新生儿脐血铅与环境因素的关系[J]. 新疆医科大学学报,2002,25(4)：394~396.

[17]Li Xia，Xin Yu， Zhang Guangxing. Air Pollution Characteristics of Multi-cities in the north of middle Tianshan Mountain, Xinjiang, China. The 3rd International Conference on Bioinformatics and Biomedical Engineering (iCBBE 2009).

[18]周国兵，王式功. 重庆市主城区空气污染天气特征研究[J]. 长江流域资源于环境，2010,19(11)：1349~1345.

[19]王式功，杨德保，陈长和. 兰州市不同季节大气污染物时空变化规律的对比分析[J]. 兰州大学学报(自然科学版)，1994，30(3)：150~155.

[20]田裘学，周伶芝，王瑞，等. 兰州市空气污染物的变化规律与特征[J]. 中国环境监测，2001，17(特刊)：14~18.

[21]穆珍珍，赵景波，徐娜，等. 西安市雁塔区冬季可吸入颗粒物时空变化研究[J]. 环境科学学报，2011，31(7)：1509~1516.

[22]孙玫玲，穆怀斌，吴丹朱，等. 天津城区秋季PM2.5质量浓度垂直分布特征研究[J]. 气象，2008，34(10)：60~66.

[23]王京丽，谢庄，张远航，等. 北京市大气细粒子的质量浓度特征研究[J]. 气象学报，2004，62(1)：

104~111.

[24]王淑英，张小玲．北京地区PM10污染的气象特征[J]．应用气象学报，2002，13(特刊)：177~184.

[25]陈彬彬，林长城，杨凯，等．福州市大气污染时空变化及其与气象条件关系[J]．环境科学与技术，2009，32(6)：125~132.

[26]张海霞，董占强，杨玲珠，等．邯郸市可吸入颗粒物的污染现状及相关气象条件分析[J]．气象与环境科学，2009，32(增刊)：134~137.

[27]杨静，武疆艳，李霞． 乌鲁木齐冬季大气边界层结构特征及其对大气污染的影响[J]．干旱区研究，2011，28(4)：718~723.

[28]段欲晓，徐晓峰．北京地区污染特征及气象条件分析[J]．气象科技，2001，28(4)：11~14.

[29]吉东生，王跃思，孙扬，等．北京大气中SO_2浓度变化特征[J]．气候与环境研究，2009，14(1)：69~76.

[30]北京市环境保护局．2006．1997~ 2006 年北京市环境状况公报[EB/ OL] .

[31]冉靓．上海地区与天津地区地面臭氧光化学研究[D]．北京：北京大学物理学院，2012.

[32]安俊琳，王跃思，李昕，等.北京大气O_3与NO_x的变化特征[J]．生态环境，2008，17(4)：1420～1424 .

[33]中华人民共和国气象行业标准霾观测和预报等级．北京，气象出版社，2010.

Effects of meteorological conditions on high BC concentration at Xi'an from 2003 to 2007

（Zhao Shuyu[1]）

1 Institute of Earth Environment, Chinese Academy of Sciences, Xi'an China, 710075

Abstract This study mainly investigated the causes of high black carbon (BC) episodes and effects of meteorological conditions on air quality in winter at Xi'an. Continuous BC mass concentration was measured from September 2003 to August 2007 at the site of Institute of Earth Environment, an urban site at Xi'an. Averaged BC concentrations were higher in winter and autumn than those in summer and spring. High BC concentration often appeared in winter and the magnitude was higher than those measured at other urban sites. Annual averaged BC concentration showed a linear decline that indicated the reduction of emissions and proportion of coal burning in the total energy consumption in winter. Relationships between BC concentration and meteorological conditions showed that an inversion layer, descending motion in the low troposphere and weak surface wind jointly contributed to high BC concentration in winter at Xi'an. Significant negative relationships between BC concentration and boundary layer height, wind speed implied that meteorological conditions directly affected seasonal variation of BC concentration. Additionally, less precipitation was also a key factor that led to high BC concentration in winter at Xi'an due to BC accumulation in the atmosphere.

Keywords: BC, Xi'an, boundary layer height, wind speed, precipitation

大气边界层中 VOCs 层化分布与逆温现象之相关性探讨

（郑佳俊[1] 林启灿[2] 袁中新[3] 洪崇轩[4] 廖思婷[1]）

[1] 高雄海洋科技大学海洋环境工程系(所)硕士生

2 高雄海洋科技大学海洋环境工程系(所)教授

3 中山大学环境工程研究所教授

4 高雄第一科技大学环境与安全卫生工程系助理教授

摘　　要：VOCs 是产生臭氧空气质量污染物之前驱物，大气中 VOCs 浓度可能会受到气象条件影响，而产生层化现象；过去也有许多文献提出，大气中有逆温层、混合层等情况出现时，会导致大气成份的层化分布。然而，臭氧空气质量模式推估，长期以来皆假设前驱污染物在垂直高度范围是均匀混合；为印证大气逆温层化现象是否会导致 VOCs 层化分布，本研究监测大气边界层中 VOCs 浓度之垂直分布，并与逆温现象之相关性进行探讨，以供空气质量模式研究人员评估其可能会导致的推估误差。研究选用探空气球采样法，进行从地面至垂直高空 800 公尺间，大气温度量测与气体采集，并以热脱附冷冻装置做为前处理再搭配 GC/MSD 进行 VOCs 之检验工作。

研究显示，冬季大气温度稳定度日夜变化结果，白天时段先由中性稳定转至极不稳定的状态，再逐渐回转至中性弱稳定；夜间时段，在 21:00-23:00 之间，大气稳定度为极稳定，此时亦是逆温层容易出现之时段；冬季逆温层是以辐射逆温为主，且高度范围较接近地面在 200-500 公尺之间。夏季大气稳定度趋势变化与冬季相反，逆温层则容易出现在白天 07:00-10:00 间，出现高度范围变化也较大。当逆温层出现时，有观察到污染物会蓄积在逆温层下方之现象，符合逆温现象不利污染物垂直扩散之预期；另外，也观察到逆温层上方有高浓度出现，此现象可能是远程传输之污染所导致。

关键字：挥发性有机化合物（VOCs），逆温层，层化现象，臭氧空气质量，探空气球

探寻 IMPROVE 和 NIOSH 法元素碳（EC）测定结果的数学联系

（支国瑞[1]，陈颖军[2]，李洋[1]）*

（[1]中国环境科学研究院，[2]中科院烟台海岸带研究所）

元素碳（EC）指大气气溶胶中有一定耐热作用的吸光碳，源于含碳物质的不完全燃烧，既是一种空气污染物，又是一种重要的气候影响因子。30 多年来，实践中出现了多种测定方法，但由于不同方法着眼于 EC 的不同性质，造成测定结果的较大差异，为基于 EC 测定的排放清单制定、空气污染模拟及气候效应评估带来极大不便。即使是目前较为普遍使用的两种热光法测定协议，即 IMPROVE 和 NIOSH（表 1），其 EC 测定结果的差异也很明显。因此建立方法间的数学联系，对于不同方法的数据共享具有重要的理论和实践意义。

表 1. NIOSH 和 IMPROVE 分析程序

		NIOSH[a]		IMPROVE[b]	
载气	碳化分	温度 (ºC)	时间 (s)	温度 (ºC)	时间 (s)
He	OC1	250	60	140	160~580
	OC2	450	60	280	160~580
	OC3	650	60	480	160~580
	OC4	850	90	580	160~580
	炭化校正	透射		反射	
He/O_2	EC1	550	45	580	160~580
	EC2	650	60	740	160~580
	EC3	750	60	840	160~580
	EC4	850	40		
	EC5	870	40		

[a]类似于 Birch (1998); [b]2005 年以后的 DRI Model 2001 仪器所使用的温度，每步驻留时间并不固定，但介于 160-580s 之间，依每个 FID 碳峰接近基线为准。

实验基于九种不同成熟度的煤（烟煤、无烟煤），以不同型态（煤块、蜂窝煤）在不同炉型（改进、简易）中燃烧，使用自制的烟气稀释采样系统采集烟气的颗粒物于石英滤膜上，共得到 27 个滤膜样品，分别进行 NIOSH 法和 IMPROVE 法的 EC 测定。以测定结果建立如图 1 的坐标体系，X 轴为 IMPROVE 法测得的 EC 与总碳（TC）的比值（$R_{EC/TC}$），y 轴为两种测定结果的相对差（$(EC_{IMPROVE}-EC_{NIOSH})/EC_{IMPROVE}$）。通观察数据的特点，初步设计了 x、y 的关系构架为 $y=(1-x)/(1+mx^n)$。使用 SPSS 统计分析软件，拟合最佳的 m 值和 n 值，最终确定经验方程 $y=(1-x)/(1+4.86x^2)$。一些其它的实验数据支持该关系的合理性，但仍需在更多地区开展大气气溶胶 EC 的实际对比，以便对此关系进行验证和改进。通过该经验方程，把来自于 NIOSH

* 联系人：支国瑞，zhigr@craes.org.cn

基金：中国自然科学基金（41173121）；国家环境保护公益性行业科研专项（201209007）

和 IMPROVE 的两种 EC 分析结果联系起来了.

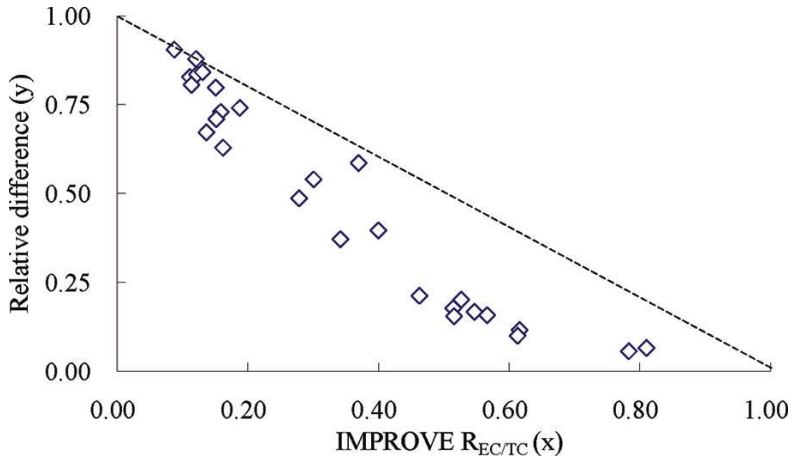

图 4 数据分布观察

主要参考文献

(1) Birch, M. E. Analysis of carbonaceous aerosols: Interlaboratory comparison. *Analyst* **1998**, 123(5), 851-857.

(2) Chow, J. C.; Watson, J. G.; Chen, L. W., et al. The IMPROVE_A temperature protocol for thermal/optical carbon analysis: maintaining consistency with a long-term database. *Journal of Air & Waste Management Association* **2007**, 57(9), 1014-1023.

(3) Chow, J. C.; Watson, J. G.; Chen, L.-W. A., et al. Comparison of the DRI/OGC and Model 2001 Thermal/Optical carbon analyzers. Prepared for the IMPROVE Steering Committee, Fort Collins, CO, by Desert Research Institute, Reno, NV. **2005**,

(4) Chow, J. C.; Watson, J. G.; Pritchett, L. C., et al. The DRI Thermal/Optical Reflectance carbon analysis system: Description, evaluation and applications in U.S. air quality studies. *Atmospheric Environment* **1993**, 27A(8), 1185-1201.

(5) Zhi, G.; Chen, Y.; Sun, J., et al. Harmonizing aerosol carbon measurements between two conventional thermal/optical analysis methods. *Environmental Science & Technology* **2011**, 45(7), 2902-2908.

利用 CALIPSO 星载激光雷达资料研究我国 PM10 浓度分布特征

（周天，黄忠伟）

兰州大学大气科学学院 半干旱气候变化教育部重点实验室，甘肃，兰州 730000

摘要：气溶胶显著的环境和气候效应使其成为影响环境和气候重要且不确定的因素之一。近年来，可吸入颗粒物 PM10 对我国区域环境和气候的影响引起人们越来越多的关注。本文基于 CALIPSO 星载激光雷达可提供全球尺度气溶胶垂直结构和光学特性的优势，综合分析了 2009 年 1 月至 2013 年 2 月期间的 CALIPSO 卫星资料与台湾中坜站（24.95°N,121.22°E,135 米）PM10 观测资料的关系。首先，利用统计学方法建立中坜站地区气溶胶层积分衰减后向散射系数、层积分退偏比和层积分色比与 PM10 浓度分布的关系，初步结果显示该地区气溶胶光学特性与 PM10 浓度分布有很好的相关性；其次，将该关系推广至全国地区，初步取得了我国 PM10 浓度的地域分布特点；然后，分析不同区域 PM10 浓度分布的月变化、季节变化和年际变化规律，进一步深入了解我国不同地区 PM10 浓度的时空分布特征。本文研究结果不仅表明 CALIPSO 星载激光雷达在环境研究领域的独特优势，而且获取我国 PM10 浓度的时空分布特征，可为全球气候变化和环境科学等相关研究提供重要的观测资料。

关键词： CALIPSO，星载激光雷达，PM10

Investigations of the Chemical Characteristics from an Intensive Sainampling of Ambient Particles in Shanghai, China

（Chong-shu Zhu[1], Jun-ji Cao[1,2]）

[1] *Key Laboratory of Aerosol，SKLLQG, Institute of Earth Environment, Chinese Academy of Sciences, Xi'an, China*

[2] *Institute of Global Environmental Change, Xi'an Jiaotong University, Xi'an, China*

Abstract

Ambient daytime and nighttime $PM_{2.5}$ and TSP samples were collected in parallel at two sites (named Pudong and Jinshan) in Shanghai, China. The samples were analyzed for carbon fractions, elements, water-soluble ions (WSIs) at both sites. The lower concentrations of particulates were found at Pudong, and higher level of $PM_{2.5}$ and TSP concentrations were observed in daytime than nighttime for both sites. The variations of chemical components (OC, EC, ions and elements) as well as the species ratios were discussed in depth for daytime and nighttime. The results showed that organic aerosol and secondary sulfate are the most abundant components of the particle, and the contributions were variable during the different sampling periods due to the strength of local emission and the secondary production. The discussion indicated that the particulates were variable for different areas according to the local emissions and meteorology. The results can give some indications for the developing effective strategies for urban sub-zone pollution control.

Keywords: $PM_{2.5}$, TSP, carbonaceous fractions, ions, elements, Shanghai

大气细颗粒物对人体健康的影响

（朱彤）

北京大学环境科学与工程需要，环境与健康研究中心

摘　要：粒径小于 2.5 微米的大气细颗粒物(PM2.5)对人体健康有显著的危害。目前我国多个城市 PM2.5 超标严重，引起了社会和公众的广泛关注，已成需要重点控制的大气污染物。尽管大量的流行病学和毒理学研究证实大气污染与心肺系统疾病发病率和死亡率增加显著相关，但对于大气颗粒物的理化性质与健康效应之间的关系仍不清楚，其危害机制亟待深入研究。为全面探索污染物对于心血管呼吸系统、机体代谢和免疫等功能的影响，现代流行病学加速了与暴露组学、临床诊治、基因组学等学科的结合，在人群调查中采用生物标志技术追踪污染物的暴露和代谢途径、分析污染物中的关键化学组分对于靶器官及组织的影响及交互作用机制。

流行病学研究显示空气污染是呼吸系统和心血管疾病的重要危险因素，但人群研究的直接证据不足。目前主要的假设为空气污染首先诱发呼吸道局部氧化应激和炎症，进而导致全身性炎症和氧化性损伤，促进导致血栓形成、引发上皮细胞损伤、引发心脏自主神经功能和血管功能异常。2008 年北京奥运会和残奥会期间实施了大量的空气污染控制措施，奥运会前后大气污染水平发生急剧变化，为检验这些假设提供了难得的的实验契机。北京大学和美国数所大学的研究人员在北京奥运前、中、后五个月密集追踪了 125 名健康年轻人的系统性炎症和血栓形成等生物性标记物水平的变化。检测的指标包括呼吸道炎症水平（FeNO）、呼吸道氧化应激素水平（EBC Nitrite Nitrate）、DNA 损伤（8-OHdG）、全身炎症（纤维蛋白原、C-反应蛋白 CRP、白细胞 WBC 计数）、血栓形成或内皮功能障碍(可溶性血小板选择蛋白 sCD62P、可溶性 CD40 配基 sCD40L、血管假性血友病因子 vWF）等有关的生物性标记物，以及心率、血压等。结果显示北京奥运期间空气污染物水平与健康年轻人呼吸道炎症水平、呼吸道氧化应、DNA 损伤、血栓形成的生物标志物、心血管生理学指标的急性改变相关。

在奥运期间同期进行的患心血管疾病的老年人群追踪观测和小学儿童人群追踪观测。结果显示，大气细颗粒物及气态污染物暴露后数小时内，污染物浓度增加与呼吸系统炎症、交感/副交感神经功能的降低和血压的升高具有显著关联；全身低炎症水平和肥胖可能进一步加剧污染物急性暴露的心血管功能损伤；细颗粒物中的黑碳(Black Carbon)对于呼吸系统炎症和心血管健康的影响最为显著。

武汉市道路一侧 $PM_{2.5}$ 和 PM_{10} 浓度监测

（朱颖，李可，刘彬，向荣彪）

华中农业大学资源与环境学院，武汉 ，430070

摘　要：在2012年8月和10月采用重量法和PM质量分析仪对武汉市南湖大道一侧的PM_{10}和$PM_{2.5}$进行了阶段性监测，并与华中农业大学内PM_{10}和$PM_{2.5}$浓度进行对比。结果表明，南湖大道8月监测期间PM_{10}和$PM_{2.5}$平均浓度分别达到137.2μg/m^3，61.4μg/m^3；超标率分别高达57%，57%；10月监测期间PM_{10}和$PM_{2.5}$平均浓度分别达到187.4μg/m^3，100μg/m^3；超标率分别高达83%，75%，污染较为严重。通过PM_{10}和$PM_{2.5}$小时平均浓度日变化趋势分析，发现上午9时及晚上9时PM_{10}和$PM_{2.5}$浓度出现峰值，下午2时至3时空气质量相对较好。

关键字：PM_{10}，$PM_{2.5}$，超标率

气溶胶对全球气候变化和人类健康的的影响逐步受到广泛关注。PM_{10} 和 $PM_{2.5}$ 是气溶胶的重要组成部分，是目前大气环境质量评价中一个重要污染指标。早在 1997 年美国环保署(EPA)便认为 PM_{10} 和 $PM_{2.5}$ 为代表性最强、危害最大的大气污染物。并在空气质量标准中明确规定了 PM_{10} 和 $PM_{2.5}$ 的浓度限值（NAAQS,2006）。我国最近修订的环境空气质量标准也将 $PM_{2.5}$ 纳入常规空气质量评价的范围。中国近年来随着大气污染的日趋严重，我国多个大城市，如北京、上海、珠江三角洲等地，均陆续开展了 PM_{10} 和 $PM_{2.5}$ 的相关监测[1]。研究表明，机动车排放为大气颗粒物的主要来源之一，道路两侧的空气污染不容忽视。但武汉地区相关监测研究甚少。因此，本文选取南湖大道路口一侧对 PM_{10} 和 $PM_{2.5}$ 污染水平进行了监测，以期为武汉市 PM_{10} 和 $PM_{2.5}$ 控制提供基础数据。

1材料与方法

1.1 监测点

武汉市洪山区南湖大道是贯穿南湖延岸的主要交通干线，西起与李纸路交汇处，东到与光谷大道的交汇处，是连接南湖花园城与武汉市光谷高新技术开发区的主要干道。选取南湖大道某交通路口一侧作为监测地点。该监测点南接华中农业大学，北临南湖，东西向为交通路段，行车量中等，周边无大型工地或工厂，基本无局地建筑活动。同时取华中农业大学校园内标本馆楼顶作为参比监测点。周边为教学区，交通工具以非机动车为主，无局地建筑活动，无典型污染源。

1.2 仪器和方法

采样器为智能中流量大气采样器（TH-150A，武汉天虹仪表有限责任公司），流量为100L/min；切割器为 PM_{10}-PM_5- $PM_{2.5}$ 串级大气颗粒物切割器（武汉天虹仪表有限责任公司），使用该切割器的 PM_{10} 和 $PM_{2.5}$ 切割头分别进行 PM_{10} 和 $PM_{2.5}$ 的样品采集。采集所用滤膜为聚丙烯滤膜。采样前后将滤膜置于干燥器中恒温恒湿 24 小时，并用万分之一天平进行滤膜

称重。采样前后滤膜质量之差除以采样时标准状态下体积得到颗粒物 24 小时平均浓度。此外，连续监测采用 PM 质量分析仪（PM-325, HCT Inc., Korea）。

2012 年 8 月和 10 月在南湖大道一侧各进行了为期 11 天的监测。9 月在标本馆处监测 12 天。其中，PM 质量分析仪于每日 6 时连续监测至凌晨零点，中流量采样器进行 24 小时连续采样。

2.结果与讨论

2.1 PM_{10} 和 $PM_{2.5}$ 污染水平

表 1 为 2012 年 8 月和 10 月南湖大道 PM_{10} 和 $PM_{2.5}$ 的日均浓度范围及超标率，以及标本馆 PM_{10} 和 $PM_{2.5}$ 的日均浓度范围及超标率。超标率参考《环境空气质量标准》（GB3095-2012）中二级标准 PM_{10} 的 24 小时浓度限值（150μg/m^3），$PM_{2.5}$ 的 24 小时浓度限值（75μg/m^3）计算所得。可以看出，标本馆 PM_{10} 和 $PM_{2.5}$ 浓度整体低于 8 月和 10 月在南湖大道路口上的 PM_{10} 和 $PM_{2.5}$ 浓度。分析两处环境特点知：南湖大道地处交通要道，空气流动性良好，但往来车辆以机动车为主，植被覆盖率低于校园内；标本馆于校园区内，周边为教学区，植被覆盖率较高，空气流动性良好，且交通工具以非机动车为主。因此，机动车辆尾气排放和地面扬尘可能是造成南湖大道 PM_{10} 和 $PM_{2.5}$ 浓度较高的主要原因。此外，监测期间 8 月、9 月平均温度分别为 31.8℃，29.6℃，10 月平均温度为 19.7℃。

比较三次监测：8 月，9 月天气都较为湿热，不同在于采样点周边环境。因此，机动车辆尾气排放和地面扬尘均可能是南湖大道路口 PM_{10}，$PM_{2.5}$ 浓度高于校园内的主要因素。而 8 月和 10 月南湖大道上的两次监测，8 月明显优于 10 月。其主要原因可能是 8 月雨水较多，温度较高，风速高于 10 月，空气流动性稍强，从湖面带来洁净空气，均对大气颗粒物污染的稀释起一定的作用。

表 1　PM_{10} 和 $PM_{2.5}$ 浓度及超标率

Table 1　Summary of PM_{10} and $PM_{2.5}$ Pollution

监测点		样品数	$PM_{2.5}$ 浓度范围 (μg/m^3)	$PM_{2.5}$ 平均浓度 (μg/m^3)	$PM_{2.5}$ 超标率(%)	PM_{10} 浓度范围 (μg/m^3)	PM_{10} 平均浓度 (μg/m^3)	PM_{10} 超标率(%)
标本馆		11	34.5 ~ 179.9	53.6	57	57.0 ~ 220.5	117.1	57
南湖大道	8 月	11	27.6 ~ 116.2	61.4	57	128.2 ~ 341.2	137.2	57
	10 月	12	57.9 ~ 143.5	100.0	75	127.2 ~ 309.3	187.4	83

2.2　PM_{10} 和 $PM_{2.5}$ 浓度日变化

表 2 给出了监测期间一天内的温度及风速范围，并统计了总降雨量。且一天内上午 6 时左右温度最低，日出后温度逐渐升高，至午后 15 时左右达最高温度，之后温度又逐渐下降。相对湿度变化趋势与温度变化趋势相反。风速变化无明显规律。图 2 和图 3 对一天内 6

点至 24 点，两次采样中 PM_{10} 和 $PM_{2.5}$ 浓度逐时变化进行了比较。由图中可看出，PM_{10} 和 $PM_{2.5}$ 在一天内随时间变化趋势都呈现较高的一致性。

从整体上看，8 月气温明显高于 10 月，而 PM_{10} 和 $PM_{2.5}$ 浓度整体低于 10 月，可能是因为温度上升可以促进大气近地层的垂直对流，利于污染物扩散[2,3]，在其他影响因素差别不大的条件下，温度成主要影响因素。值得注意的是，从日变化趋势上看，PM_{10} 和 $PM_{2.5}$ 呈现先高后低再高的变化趋势。在气温逐步上升的早晨 9 时左右，PM_{10} 和 $PM_{2.5}$ 浓度会有平缓上升，可能是因为早 6 时到 9 时，南湖大道上的车流量明显成正增长，此阶段的大气颗粒物主要来源于机动车的排放，车流量成为浓度变化的主导因素。而后在日照充足且气温较高的下午 2 时至 3 时，PM_{10} 和 $PM_{2.5}$ 浓度达到一天内最低。此时为一天内温度最高，湿度最低的时段，大气层结相对不稳定，利于污染物的扩散。在车流量无大幅度变化的情况下，温度和湿度再次成为 PM_{10} 和 $PM_{2.5}$ 浓度变化的主要影响因素。日落后至夜间， PM_{10} 和 $PM_{2.5}$ 浓度又再次回升，可能是因为日落后空气湿度大幅上升，风速小，温度虽有降低但仍湿热，这样的气象条件常常导致 PM_{10} 和 $PM_{2.5}$ 浓度的持续积累 [4]，使得 PM_{10} 和 $PM_{2.5}$ 浓度有小幅上升。

表 2 各监测期间温度、湿度、日降雨量及风速

Table 2 The temperature, humidity, air speed and daily rainfall

监测点		温度℃	风速 m/s	湿度%	降水量 mm
南湖大道	8 月	27.4 ~ 32.8	0.33 ~ 0.81	25 ~ 98	3.45
	10 月	17.6 ~ 23.7	0.03 ~ 0.67	45 ~ 83	3.19

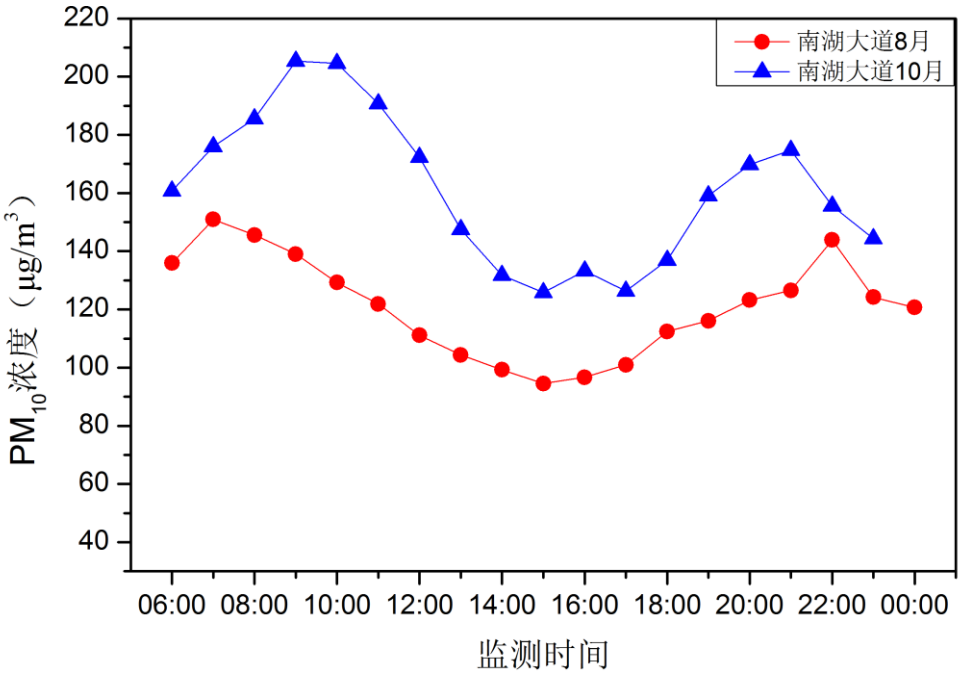

图 2 PM_{10} 逐时变化

Fig.2 Hourly variation of PM_{10} mass concentration

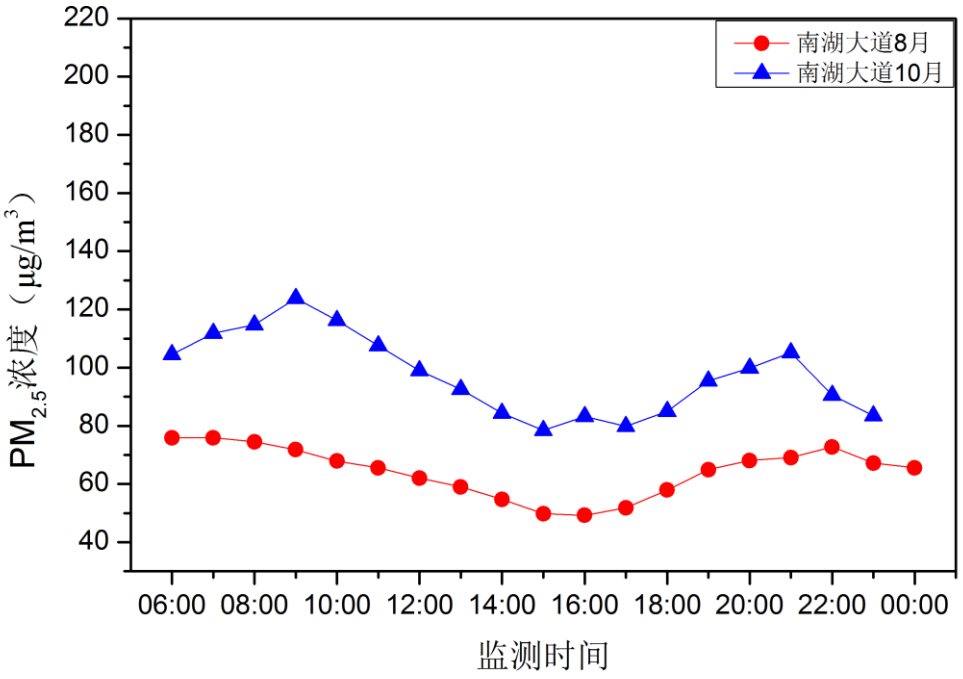

图 3 $PM_{2.5}$ 逐时变化

Fig.3 Hourly variation of $PM_{2.5}$ mass concentration

3 结论

2012 年 8 月和 10 月，在南湖大道路口一侧监测 PM_{10} 和 $PM_{2.5}$ 污染情况。发现南湖大道上污染超标较为严重，超标率高于 50%。并与校园内 PM_{10} 和 $PM_{2.5}$ 浓度相比，南湖大道监测点浓度较高，主要原因可能是机动车辆尾气排放和地面扬尘对南湖大道有较多贡献。

在 PM_{10} 和 $PM_{2.5}$ 逐时变化中，从早上 6 时开始，呈现先高后低再高的变化趋势，其中在下午 2 时至 3 时浓度最低，相反早晨和晚间的 PM_{10} 和 $PM_{2.5}$ 浓度较高。

参考文献

[1]. 魏复盛, 滕恩江, 吴国平, 胡伟, W. E. Wilson, R. S. Chapman, J. C. Pau, J. Zhang. 我国4个大城市空气 $PM_{2.5}$、PM_{10}污染及其化学组成. 中国环境监测, 第17卷特刊, 2001-1.

[2]. 宋宇, 唐孝炎, 张远航, 等. 夏季持续高温天气对北京市大气细粒子($PM_{2.5}$)的影响[J]. 环境科学, 2002, 23(4): 33-36.

[3]. Whiteaker J, Suess D, Prather K. Effects of meteorological conditions on aerosol composition and mixing State in Bakersfield, CA[J]. Environmental Science and Technology, 2002, 36(11): 2345-2353.

[4]. 徐敬, 丁国安, 颜鹏, 王淑凤等. 北京地区 $PM_{2.5}$的成分特征及来源分析; 应用气象学报, 第 18 卷 5 期, 2007-10.

Comparing new particle formation events between in highly and less polluted atmosphere: Implication of a critical role of anthropogenic pollutants in growing new particles to CCN size

*（Y.J. Zhu[1], H.W. Gao[1], Z.Q. Duan[1], G.J. Evans[2], X. H. Yao[*12]）*

[1]Key Lab of Marine Environmental Science and Ecology, Ministry of Education, Ocean University of China, Qingdao 266100, China

[2]Southern Ontario Centre for Atmospheric Aerosol Research, University of Toronto, Canada

**Corresponding authors: Email: xhyao@ouc.edu.cn, Tel: 86-532-66782565, fax 1-831-618-6654,*

Abstract

When new particles formed in the atmosphere grow over 50-80 nm, they can be activated as cloud condensation nuclei (CCN) and lead to an increase of cloud albedo. Knowledge gaps still existed, e.g., 1) in what type of new particle formation (NPF) events new particles can grow over 50 nm? 2) which chemicals determine the growth of new particles to be over 50 nm? In this study, NPF events were investigated at two urban sites, in Qingdao and in Toronto, using two identical Fast Mobility Particle Sizer (FMPS) in spring. The satellite column density of pollution gases and the particular chemical concentration in $PM_{2.5}$ both showed much higher concentrations of anthropogenic air pollutants in Qingdao than in Toronto. NPF events were observed in 16 days out of 39 sampling days in Qingdao and 13 days out of 31 sampling days in Toronto. The occurrence frequency of NPF events between Qingdao (41%) and Toronto (43%) was comparable to each other. In Qingdao, the geometric mean diameter of grown nucleated particles ($D_{pg,i}$) in 15 days grew to larger than 40 nm except in one day when the growth of new particles terminated at ~20 nm. In addition, new particles in 8 days out of the 15 days partly or entirely grew over 50 nm and they could even reached 100 nm in two days. Two-phase growth was generally observed in these NPF events of Qingdao. The first-phase growth occurred in daytime and the CMAQ modeling results suggested that formation of secondary organics was likely the major cause for the growth. The second-phase growth was observed at night and was associated with the increased concentrations of NH_4^+ and NO_3^-, implying that NH_4NO_3 condensation played an important role in the growth. In Toronto, NPF events in 4 days followed with the growth of new particles <~20 nm while new particles grew up to ~40 nm in the remaining NPF events. A slight growth of new particles at night was observed only in 3-days NPF events when the increased concentrations of NH_4^+, NO_3^- or the increased relative humidity were observed. However, the calculated $D_{pg,i}$ was less than 45 nm for all NPF events in Toronto, implying a negligible contribution of new particles to the population of CCN.

Key words: nucleation, particle growth, anthropogenic pollutants, NH_4NO_3 condensation

Characterization of Springtime Atmospheric Organic and Elemental Carbon of $PM_{2.5}$ in a Typical Semi-Arid Area of Northeastern China

（Renjian Zhang[1], Jun Tao[2], K.F. Ho[3,4], Zhenxing Shen[5]）*

[1] RCE-TEA, Institute of Atmospheric Physics, Chinese Academy of Sciences, Beijing 100029, China

[2] South China Institute of Environmental Sciences, Guangzhou 510655, China

[3] SKLLQG, Institute of Earth Environment, Chinese Academy of Sciences, Xi'an 710075, China

[4] School of Public Health and Primary Care, The Chinese University of Hong Kong, Hongkong, China

[5] Department of Environmental Science and Engineering, Xi'an Jiaotong University, Xi'an 710049, China

ABSTRACT： Daily particulate matter ($PM_{2.5}$) aerosol samples were collected in Tongyu, a semi-arid area in northeastern China in spring. The concentrations of organic carbon (OC) and elemental carbon (EC) were determined with a thermal/optical carbon analyzer in the filter samples. The average concentrations of OC and EC in $PM_{2.5}$ were 14.1 ±8.7 and 2.0 ±1.3 μg/m^3, respectively. A good correlation between OC and EC was observed during the spring season, suggesting that they might be derived from similar sources. The correlation between OC and K^+ was high (R = 0.74) and the K^+/OC ratio, as determined from their linear regression slope, reached 2.57. The good correlation and the high K^+/OC ratio indicated that biomass-burning was probably one of the major sources of OC in this region. The concentrations of estimated secondary organic carbon (SOC) in $PM_{2.5}$ in Tongyu ranged from below detection limit to 26.1 μg/m^3 (mean, 5.9 μg/m^3). The percentages of SOC in OC and in $PM_{2.5}$ mass were 42.0% and 2.1%, respectively. The SOC concentrations during dust storms (DS) periods were higher than those during non-dust storm (NDS) periods, suggesting that chemical reaction processes involving gas-particle conversion should have occurred during the long-distance transport of aerosol particles.

Keywords: Semi-arid area; Organic carbon; Elemental carbon; Dust storm.

直接称量法环境空气颗粒物自动监测系统

摘　要：本文提出了一种新的环境空气颗粒物 PM2.5 自动监测方法——直接称量法。着重介绍了实现这种方法的仪器结构组成、工作原理、数据发布方式以及为提高称量精度而设立的标准化的称量环境。通过仪器的原理和工作过程描述论证了这种方法具有更高的准确性；通过初步监测数据证明这种系统具有良好的稳定性和一致性。作者认为这种监测 PM2.5 含量的直接称量法就是基础验证法的自动化和智能化，或者说是自动化和智能化的基础验证法。它消除了现行的间接监测方法的量值转换误差，是一种更科学、准确的环境空气颗粒物自动监测的方法，具有广阔应用和推广前景。

Real-time Measurements of Secondary Organic Aerosol from the Photooxidation of Naphthalene using Single Particle Mass Spectrometry

（ang Chen[1, 2], Robert M. Healy[2], Shouming Zhou[2], and John C. WengYer[2]）

[1]Insitute of Earth Environment, Chinese Academy of Sciences, Xi'an China

[2]Department of Chemistry and Environmental Research Institute, University College Cork, Cork, Ireland

Naphthalene is the most abundant polycyclic aromatic hydrocarbon detected in urban air and has recently been identified as an important precursor for the formation of secondary organic aerosol (SOA) in the atmosphere. In this work, a series of simulation chamber experiments has been performed on the photooxidation of naphthalene under a variety of reaction conditions. The decay of naphthalene was monitored using in situ FTIR spectroscopy and the formation and evolution of SOA was followed using a scanning mobility particle sizer. An Aerosol Time-of-Flight Mass Spectrometer (ATOFMS) was used to determine the chemical composition of the SOA in real-time. In experiments using NOx as the hydroxyl radical precursor, the single particle mass spectra were found to change slowly over a period of hours. The positive ion mass spectra initially contained hydrocarbon fragments typical of aromatic species which are tentatively attributed to ring-retaining oxidation products such as naphthol and nitronaphthalene. After 3-4 hours the intensity of the hydrocarbon fragments was significantly reduced and the negative ion mass spectra displayed characteristic features of oxidized organic aerosol and nitrates. Interestingly, some of these peaks continued to increase after the lights were turned off, suggesting that particle phase processing was maintained, even under dark conditions. The results from these experiments indicate that ATOFMS can be used to monitor chemical changes in SOA in real-time and is a potentially useful tool for investigating aerosol formation and ageing.

Keyword: Secondary Organic Aerosol, Naphthalene, online single particle mass spectrometer.

半干旱区气溶胶物理特性的观测研究

（张武 冯岚 李娜 颜娇珑 王雅萍 柳丹 黄晨然）

半干旱气候变化教育部重点实验室 兰州大学大气科学学院，兰州，甘肃，730000

摘　要:本文利用兰州大学半干旱气候与环境观测站(SACOL)在 2010 年 1 月-2011 年 2 月观测数据，分析了气溶胶光学参数、不同粒径段气溶胶数浓度和数谱分布随时间变化的特点，以及气象条件对这些参数的影响，讨论了 AOD 与 PM_{10} 质量浓度的相关性。同时，探讨了用 APS 资料拟合 PM_{10} 质量浓度的方法，结果表明：

SACOL 站气溶胶光学厚度、浑浊度系数的年均值分别为 0.410 和 0.231，季节平均值按春、冬、夏、秋顺序依次减少，波长指数的年均值 0.840，季节平均值则按春、冬、夏、秋依次增大。

SACOL 站大气中气溶胶总数浓度主要取决于 $PM_{2.5}$ 数浓度，特别以粒径小于 1.0□□的积聚模态居多，其中冬季粒径小于 1μm 的气溶胶粒子数浓度又远远超出其它季节。

SACOL 站常年盛行东南和西北风，这两个方向的上风向为兰州市和榆中县，是人口聚集区，人类活动产生的气溶胶被输送到下游，气溶胶粒子数浓度出现高值的频次最多。

2010 年春季，SACOL 站所在区域沙尘天气频繁发生。沙尘天气中，AOD 增大，浑浊度系数与 AOD 变化趋势保持一致，呈正相关关系，波长指数与它们呈较弱的负相关。沙尘暴发生前，$PM_{2.5}$ 数浓度急剧增大，气溶胶总数浓度主要取决于粒径小于 0.523μm 的颗粒物数浓度；沙尘暴出现时，PM_{coarse} 数浓度急剧增加，PM_{total} 质量浓度主要取决于 PM_{coarse} 数浓度。

用APS数据拟合PM_{10}质量浓度的方法中，多元线性回归在春季沙尘天气和冬季污染天气条件下的相关系数超过0.950，

关键词：气溶胶光学厚度，Angstrom 参数，粒径分布，半干旱区，SACOL

长三角臭氧和细颗粒污染及其对区域污染控制和污染-气候相互作用的启示：SORPES 观测站最新进展

（丁爱军[1]，符淙斌[1]，杨修群[1]，孙鉴泞[1]，聂玮[1]，谢郁宁[1]，齐西蒙[1]，E. Herrmann[1,2]，T. Petäjä[2]，V.-M. Kerminen[2]，M. Kulmala[2]）

[1] 南京大学气候与全球变化研究院/大气科学学院

[2] Dept. of Physics, University of Helsinki, Finland

摘　要:南京大学气候与全球变化研究院与芬兰赫尔辛基大学合作于 2009 年起在南京大学仙林校区建立和发展了地球系统区域过程观测试验基地（SORPES），该基地致力于研究地表物理过程、大气化学-气候相互作用、生态系统-大气相互作用和水文过程及水循环。站点位于南京东郊、长三角西部的下风向区域背景地区，具有很好的区域代表性。通过近 2 年的连续观测，本研究获得了长三角西部地区臭氧和细颗粒物 $PM_{2.5}$ 及其相关前体物的季节变化特征，发现了该地区臭氧、细颗粒污染的重要控制因子、天气过程及区域相互影响。本研究还发现在长三角地区高污染环境下也能出现频繁的新粒子生成事件，并提出了区别于国外清洁环境的主要限制因子。研究同时发现该地区不同类型来源的高浓度颗粒物污染会实质性的改变天气乃至区域气候。2012 年 6.10 观测到的秸秆燃烧引起的高浓度气溶胶污染会导致天气预报对气温的严重高估和降水的“误报”，多种计算机模型均不能重现该极端污染天气条件下的实际气温和降水分布。秸秆燃烧烟羽与城市及区域人为污染的混合，进而通过复杂的大气边界层-污染-云和辐射的正反馈机制影响大气结构以及降水。基于此，课题组将于 2013/14 两年在生物质燃烧的多发季节在 SOEPES 站点进行两期加强观测，针对此问题进行进一步研究。

关键词：SORPES 观测基地，区域代表性，生物质燃烧，反馈机制，新粒子生成

亚洲沙尘的演化和非均相光化学过程研究

（聂玮[1]，王韬[2, 3]，丁爱军[1]，薛丽坤[3]，王文兴[2]）

[1] 南京大学气候与全球变化研究院/大气科学学院

[2] 山东大学环境研究院

[3] 香港理工大学土木与环境工程系

摘　要:沙尘表面的非均相化学对理解大气化学和辐射平衡至关重要。本研究于 2009 年春季在湖南衡山山顶（海拔 1269 米）进行了针对大气气体、气溶胶和气象参数的综合观测。研究目的主要关注于沙尘颗粒在传输过程中的化学演化和非均相光化学过程。观测期间捕获到两次沙尘暴个例，其中以 4 月 25-26 日发生的沙尘事件最为强烈。研究结果发现沙尘颗粒在传输过程中经历了显著的变化，二次成分（硫酸盐、硝酸盐和铵盐）在粗粒子模态有明显富集。用光化学年龄“时钟”法来量化了沙尘气团的大气反应时间，发现二次水溶性离子在沙尘颗粒上的富集随气团老化程度而显著增加。基于本次观测，我们提出了一个针对含碳酸钙沙尘颗粒的 4 步演化过程，包含了从初始排放沙尘颗粒到吸湿性物质（及酸性物质）覆盖的沙尘颗粒。此外，本研究还在沙尘暴过程的日间发现了高浓度的亚硝酸盐生成，实验室研究在近期验证的 NO_2 在 TiO_2 沙尘表面的光催化转化成 HONO 的过程是最可能的成因。本研究验证了非均相光化学反应在实际大气中的存在及其潜在的重要性。

关键词：沙尘暴，衡山，化学演化，非均相光化学

西安 2008 年冬季地表臭氧变化模拟及其主要影响因素

摘　要:模拟了西安地区 2008 年 12 月份地表臭氧的分布及时间变化，并分析影响臭氧变化的主要因素。模拟发现，西安城区冬季 12 月份地表臭氧浓度普遍偏低，最低的时段接近于 0。地表臭氧浓度的日变化表现为在 15~16 时（LT）达到日最高（~10ppb），在 7~8 时（LT）达到日最低（< 1ppb），这与观测结果相吻合。西安地区风场状况较稳定，本地 NOx 是地表大气臭氧浓度的主要决定因素，二者呈现出反相的变化规律，而冬季大气气溶胶和生物源排放对地表大气臭氧浓度的影响均很小。

Black carbon variation during a high pollution haze episode in Beijing, China

Qingyang Liu[1,3], Yanju Liu[1,2*], Yi Gao[4], Meigen Zhang[4], Renjian Zhang[4], Hui Ding[5] , Xuekui Qi[1]

[1]*Beijing Center for Physical and Chemical Analysis, Beijing, 100089, China*

[2]*Beijing Milu Ecological Research Center, Beijing, 100076, China*

[3]*College of Resources and Environment, University of Chinese Academy of Sciences, Beijing, 100049, China*

[4]*State Key Laboratory of Atmospheric Boundary Layer Physics and Atmospheric Chemistry, Institute of Atmospheric Physics, Chinese Academy of Sciences, Beijing, 100029, China*

[5]*Beijing Academy of Sciences and Technology, Beijing, 100089, China*

** Corresponding author*

E-mail: liuyanju@hotmail.com

Tel/Fax:：+86-10-8817 6969

Abstract: Black carbon (BC) aerosol is esthetically displeasing as it is responsible for the brown appearance of urban hazes. In this study, atmospheric BC aerosol was measured using an aethalometer (AE-31) at an urban location of Haidian District, Beijing from May 2012 to March 2013. A logarithmic negative correlation (R^2=0.5120) between BC and visibility suggested that BC was an important air pollution factor to affect air quality in Beijing. BC concentration showed significant seasonal variation with mean concentration varying between 4.24 μg m^{-3}(summer) to 8.14μg m^{-3} (winter). The highest daily mean concentration was recorded as high as 27.69 μg m^{-3}. The highest concentration of BC occurred during a high pollution haze episode in winter. In a clear day, BC exhibited a distinct diurnal pattern, with three maximum peaks within a day. However, BC exhibited a multi–peak diurnal pattern during haze episodes from Dec 2012 to Jan 2013. Statistical factors analysis demonstrated that emission source factors were not increased, leading to multi-peak diurnal pattern in BC variation. Additionally, Weather Research and Forecasting Model showed that the boundary layer height during haze episodes hourly varied in a similar trend with normal days. All the evidence indicated that BC exhibited a rather higgledy-piggledy diurnal pattern during haze episodes, which played a key role in the stabilization of haze formation.

Keywords: Black carbon aerosol, Haze formation, Diurnal pattern, Seasonal trend.

1 Introduction

Haze is defined by China Meteorological Administration as the weather phenomenon which leads to atmospheric visibility less than 10 km (Huang et al. 2012). It has caught extensive concern among the scientific community as its adverse effects on air quality, human health, visibility, cloud formation and global climate (Li, Shao and Buseck 2010, Xiao 2011). Haze formation is closely related to meteorological conditions and air pollution levels (Wang et al. 2006, Stock et al. 2012). Recent studies suggest that close linkage exist between $PM_{2.5}$ (particulate matter smaller than 2.5 μm in aerodynamic diameter) pollution in the atmosphere with haze formation (Lee, Kim and Kim 2006, Quan et al. 2011, Huang et al. 2012, Wang et al. 2006). And the roles of secondary inorganic ions (NO_3^-, $SO_4^{2-}$and NH_4^+) and carbonaceous species fraction in $PM_{2.5}$ were focused on their contributions to haze formation. Schichte et al. (2001) presented the patterns and trends of haze over the United States and found that the haze decline was consistent with the reductions in $PM_{2.5}$ and sulfur emissions. Chen et al. (2003) studied the haze formation in summer in the mid-Atlantic region, and evaluated the role of SO_4^{2-} in haze formation. Senaratne and Shooter (2004) found that the accumulation of diesel emissions contributed most to the appearance of brown haze in Auckland. In addition, Hou et al. (2006) investigated chemical characteristics of $PM_{2.5}$ in haze-fog episodes in Shanghai and found obvious trends variations in carbonaceous species of $PM_{2.5}$ during haze pollution episode, suggesting a likely key factor in the formation of haze.

Generally, the carbonaceous species in aerosols are classified into two categories: organic carbon (OC) and elemental carbon (EC, or black carbon, BC). OC aerosols are derived from primary source and chemical reactions between primary gaseous OC species in the atmosphere, whilst BC aerosols are mainly emitted from combustion sources (Ram, Sarin and Tripathi 2012). OC is considered as a negative climate force as it is a mainly scatter medium, whereas BC as a positive (warm) climate force as it absorbs solar radiation. Thus BC was considered as the second strongest contributor to current global warming next to carbon dioxide (Weller et al. 2013). In addition, BC may also have regional climate impacts. Menon et al. (2002) suggested that high concentration of BC in India and China is responsible for increase trend of flood in the south (India) and drought in the north (China). Furthermore, the sunlight absorption by BC could reduce visibility greatly in the atmosphere (Lin 2012, Cao et al. 2012, Zhou 2012). Owing to its porous and surface absorption nature, BC could serve as a site for chemically transforming secondary inorganic ions and

triggering cascade pollution events in the certain meteorological conditions, haze (Yang et al. 2012). Consequently, all these adverse effects of black carbon on climate induced the scientific community studies in BC emission source, behavior and variations and detrimental impacts on haze formation.

Observations of elevated BC concentration at global scales have been reported since the early

1980s (Tripathi et al. 2007, Wang 2011, Chen et al. 2008, Qin and Xie 2012). The regional scale observation results suggest that China and India are major emission sources of global BC aerosol (Qin and Xie 2012, Cao et al. 2009, Pan et al. 2011, Geng et al. 2012, Latha and Badarinath 2005, Tiwari et al. 2013, Rehman et al. 2011). Long-term measurements of BC in urban areas in China have carried out extensively (Lan et al. 2013, Wang et al. 2012). Qin et al (2012) investigated multi-year inventories of anthropogenic black carbon emissions in China and found that BC emission increased from 0.87 Tg in 1980 to 1.88 Tg in 2009 with a peak around 1995, and continually rising in the first decade of the 21 century. Besides, BC emissions in China contributed 70%–85% to those in East Asia and 50% in Asia, and accounted for averagely 18.97% of the global BC emissions in 1980-2009. Therefore, continuous measurement of BC in China could provide valuable information for further remediation of governmental policy and technology procedure on reducing BC emission. This study aims to investigate seasonal variation in aethalometer measured BC concentration at an urban Beijing site from May 2012 to March 2013, combining with its influence on air pollution and visibility. Daily BC concentration variations were also analyzed in a heavy haze episode occurred in Dec 2012-Jan 2013. This would provide a deeper insight for understanding the relation between BC and haze formation in China.

2 Method and Materials

2.1 Sampling site and weather data collection

The measurements presented in this study were registered at an urban site (N 39°56′50″7, E116°18′10″8), near a busy traffic line of Beijing. The sampling equipments were set up on the roof of an office building with height aboveground of 30 m and distance of about 30 m from a traffic roadside, west 3 ring road (Figure 1), without major industry nearby.

The weather data, including visibility and daily average of meteorological elements (RH, temperature and wind speed) during the sampling period, were downloaded from wunderground.com website. The boundary layer height was calculated by Weather Research and Forecasting Model (WRF). This model is configured to cover east part of China (26-45˚N, 102-134˚E) with 80 (S-N) *90 (W-E) grid points, a 27 km horizontal resolution centering at Central China (36˚N, 117.5˚E), and 35 vertical layers up to 10 hPa. The Runge-Kutta 3rd order time-integration scheme, Noah land surface model, Mellor-Yamada-Janjic Planetary Boundary Layer scheme, and Grell-Devenyi Ensemble Cumulus clouds scheme are used. The initial meteorological fields and boundary conditions are from NCEP Final reanalysis data with 1˚×1˚ spatial resolution and 6-hour temporal resolution. The simulation is conducted from December 2012 to January 2013.

The daily air pollution index of Beijing is from Beijing Municipal Environmental Protection Bureau (BMEPU) (http://www.bjepb.gov.cn/air2008/Air.aspx). Currently, only six pollutants including SO_2, NO_2, CO, O_3, PM_{10} and $PM_{2.5}$ are cited to the notification of API in Beijing. The grades of API are defined according to the daily standards of the above four pollutants. Daily API

is defined as: API=Max[API(SO_2), API(O_3), API(CO), API(O_3), API(PM_{10}), API($PM_{2.5}$)], where API(SO_2), API(O_3), API(CO), API(O_3), API(PM_{10}) and API($PM_{2.5}$) are the partial indexes of air pollutant SO_2, NO_2, CO, O_3, PM_{10} and $PM_{2.5}$, respectively. When $C_{i,j} \leq C_i \leq C_{i,j+1}$, API_i is defined as: where C_i is the daily average concentration of air pollutant i (i.e. SO_2, NO_2, CO, O_3, PM_{10} and $PM_{2.5}$). According to air quality daily report from BMEPU, the primary pollutant in Beijing was particulate matter all year around.

2.2 Measurement Instruments

Black carbon concentration was continuously measured using an aethalometer AE 31 manufactured by Magee Scientific USA. The aethalometer is an instrument providing a real time read out of the BC aerosol concentration in air stream. The instrument aspirates ambient air using its inlet tube. BC mass concentration was estimated by measuring the change in the transmittance of a quartz filter tape, on to which particles impinge. BC mass concentration was measured by 7-wavelength aethalometer online monitor with temporal resolution of 5 min during study period. It measured the optical attenuation (absorbance) of light from LED lamps emitting at seven wavelengths (370, 470, 520, 590, 660, 880 and 950 nm) with a typical half-width of 20 nm. These data are automatically recorded in the flash card of the instrument and displayed on the screen. The BC determination assumes that all the light-absorbing materials are composed of BC. The calibration of the flow rate was processed quarterly in the normal condition but did accordingly if the measurement became noisy during continuous operation (Lyamani et al. 2011). More details on the instrument and the principle of operation are given elsewhere (Weingartner et al., 2003).

3. Results and discussion

3.1 BC concentration and its relationship with API and visibility

The annual BC concentrations ranged from 0.72 to 27.69 μg m^{-3} with mean 5.51μg m^{-3} and standard deviation 4.43 μg m^{-3} during the sample period from May 2012 to March 2013. This mean BC value was higher in comparison with those measured in 2005 (Zhou et al. 2009) and 2008 (Pan et al. 2010), probably due to increase in BC emission sources in Beijing. Annually mean API at Wanliu Environmental Monitor Station was 89±67 in the studied period with 26.7 % exceeding Chinese air quality API limit (API=100, $PM_{2.5}$=75μg m^{-3}) frequently recorded. The daily visibility in this study was in the range of 1-30 km, with the average of 10.7 km, which was much lower than that in many other large cities in the world, indicating a serious air quality situation in Beijing (Deng et al. 2011, Park et al. 2006). Daily BC concentration significantly correlated (R=0.6207) and positively sloped with API (Figure 2), implying that BC concentration could be a sensitive indicator to air pollution level. In addition, our measured BC concentration was significantly, logarithmically and negatively correlated (R^2=0.5120) with visibility.

Table 1 shows that seasonal average BC values varied by nearly twofold, from a low value of 4.24±2.05 μg m^{-3} in summer to 8.14±6.37 μg m^{-3} in winter. The significant decreasing trends of visibility and API in summer comparing with winter was also observed at α=0.05 level. Similar

seasonal variations were also observed in urban areas in Europe (and elsewhere) but not in natural background sites where no seasonal variations were observed (Ramachandran and Rajesh, 2007). In quantitative examples, Röösli et al. (2001) reported higher magnitudes, 2.2-2.9 μg m^{-3} (for spring and summer) and 3.5-4.6 μg m^{-3} (in fall and winter), in comparison with other results (Lyamani et al., 2008, 2010, 2011), where enhancements from 2 up to 4-4.5 μg m^{-3} were observed between the summer and the winter. Similar seasonal variation features were also observed at Portuguese rural and urban environments, from 0.3 to 0.65 μg m^{-3} (spring/summer) up to 1.1-1.7μg m^{-3} (autumn/winter) in rural sites and from 1.8 to 2.7 up to 4.2-5.3μg m^{-3} in urban sites of Coimbra and Oporto (Castro et al., 1999). Based on the good correlation of BC with API and visibility, it is interesting to note that the seasonal differences in the BC concentrations may result in different weather phenomenon in Beijing. As an example, the winter in 2012 was characterized by a higher frequency of urban haze pollution episode than the rest seasons of the year and thus BC levels registered were higher, conversely, visibility was lower.

3.2 Black carbon variation during haze episodes

An attempt was made to study the diurnal variation of BC during a high pollution haze episode from Dec 2012 to Jan 2013. The average of 5 min BC value for selected day was plotted and result is shown in Figure 3. A distinct diurnal variation is observed in a normal day. Three peaks are observed, one in the morning around 07:00, others at noon around 12:00 and in the evening 19:00 local time. At the point from late night to early morning, there was a sharp increase in the BC concentration, likely due to vehicular emissions during the morning rush-hour. Primarily due to the decreased emissions raised by reduced vehicular traffic, the decrease in BC concentration was observed between 9:00 and 12:00, when the boundary layer height and wind speed remained constantly low (Figure 4). A slow increase in BC concentration at noon can also be partially explained by local human activities, such as cooking using fossil fuel. On the other hand, the steady decrease in BC concentrations after the noon peak can be attributed to the enhanced vertical and horizontal diffusion of aerosols, due to gradual increase in boundary layer height and wind speed, in addition to the relative decrease in traffic. Between 18:00 and 21:00, BC concentration was similarly high to that in the morning, attributing to evening rush-hourly traffic emission and domestic heating. The diurnal profile for BC concentrations measured in this study is very similar to those observed in other locations (Beegum et al. 2009, Baxla 2009, Lyamani et al. 2011).

In each haze episode, the diurnal profiles of BC concentrations appeared the peaks in different time (in Figure 3), seemly indicating different features in source emissions and the atmospheric boundary layer dynamics. However, daily average meteorological elements (RH, temperature and wind speed) during the selected days remained at the same level (Table 2). In addition, the hourly boundary layer height during haze episodes behaved in a similar trend in comparison with a normal day (Figure 4). Thus, another attempt was made to find source factors to affect BC

variation during a normal day and haze episodes. Figure 5 listed BC concentration distributions during a normal day and haze episodes. None of them showed the bell shaped feature with the exception of a normal distribution (Table 2 and Figure 5). The multimodal features shown in the histograms (Figure 5) gave a hint of mixed influence factors, resulted by different emission sources diurnally. Since most statistical methods were generally designed for a single influence factor, the possible multiple influence factors were necessary to be treated separately. Factors contributing to diurnal variation in BC concentrations were determined by using cumulative probability distribution method, which has been widely used in previous studies to calculate factor contributions to heavy metal contamination in soil (Sun et al. 2001, Siegal 2002). The cumulative probability distribution versus log BC during a normal day and haze episodes was calculated with different trends within the study area. Linear regression was further applied to build statistical calculations between diurnally variable BC concentrations and source factors. The statistical analysis demonstrated that four individual factors could be extracted with good correlation (R^2>0.88) to explain BC variables during a normal day and haze episodes (Figure 6). As one factor, vehicular emission is a known source of BC in urban environments (Chow et al. 2011). Subsequently, coal-burning and Chinese cooking process would contribute two more source distribution of BC variation, as being the focus of a number of studies (Zhao et al. 2007, Shores et al. 2012, Chow et al. 2011). In addition, various degree of BC was observed at a background level in the atmosphere (Cao et al. 2011, McMeeking et al. 2011). Thus four log-normal against cumulative probability liner regression models were fitted to the frequency distributions, in agreement with former discussions on the diurnal profile for BC in a normal day.

The emission sources investigation shows that source factors in the normal day resemble those in haze episodes. This implies that BC diurnal variation is generally controlled by meteorological elements, low wind shear and ventilation coefficient, in haze episodes. All observational haze days bear low visibility and high load PM, but aerosol particles in different hazes bear different compositions, morphologies, and mixing states. In the atmosphere, BC particles are commonly formed after BC is coated with sulfates, organic matter and sulfuric acid, thus enhancing the light absorption of BC element (Cao et al. 2011, McMeeking et al. 2011). Furthermore, the aging of BC particles may increase the absorption of visible solar radiation in comparison with BC element (Li et al. 2010, Xiao 2011). In our study, fresh BC emissions, after long-term residence in atmosphere, not only make the chemical transformation of aerosol particles complicated during the transport but also changed their physical properties in downwind areas. Therefore, long residence of BC in the atmosphere in haze episodes likely resulted in the stable haze formation.

4. Conclusions

In this study we have investigated BC concentrations at an urban area, Beijing, China, from May 2012 to March 2013. The daily mean BC concentrations varied from 0.72 to 27.69 μg m^{-3} with mean 5.51μg m^{-3} and standard deviation 4.43 μg m^{-3}. The seasonal average BC

concentrations ranged by nearly twofold, from 4.24±2.05 in summer to 8.14±6.37 μg m^{-3} in winter. In addition, daily BC concentration significantly correlated (R=0.6207) and positively sloped with API, thus could be an indicator of air pollution level. In addition, BC was significantly, logarithmically and negatively correlated (R^2=0.5120) with visibility, thus could be an important air pollution factor influencing air quality in Beijing.

Distinct diurnal variation of BC concentration was observed with three maximum peaks in normally clear days, two for rush hours and one for cook hours. In haze episodes, diurnal BC concentration bore a multi-peak pattern. Moreover hourly boundary layer height in all haze episodes behaved in a similar trend to a normal day. Factors contributing to diurnal variation in BC using cumulative probability distribution method indicated that emission source factors were not increased, leading to the increase of BC concentration. In conclusion, long residence of BC in the atmosphere in haze episodes likely resulted in the stable haze formation.

Acknowledgements

Financial supports for this work have been provided by Natural Science Foundation of China (No.41175104), the Chinese Academy Sciences "Predicted model development in haze formation" (XDB05030103) the Earmaked Fund of State Key Laboratory of Atmospheric Boundary Layer Physics and Atmospheric Chemistry, CAS.

References

Beegum, S. N., K. K. Moorthy, S. S. Babu, S. K. Satheesh, V. Vinoj, K. V. S. Badarinath, P. D. Safai, P. C. S. Devara, S. Singh, Vinod, U. C. Dumka & P. Pant (2009) Spatial distribution of aerosol black carbon over India during pre-monsoon season. *Atmospheric Environment,* 43, 1071-1078.

Cao, J.J., Q, Y. Wang, J. C. Chow, J. G. Watson, X.X. Tie, Z.X. Shen, P. Wang & Z.S. An (2012) Impacts of aerosol compositions on visibility impairment in Xi'an, China. *Atmospheric Environment,* 59, 559-566.

Cao, J.J., C, S. Zhu, J. C. Chow, J. G. Watson, Y. M. Han, G, H. Wang, Z.X. Shen & Z.-S. An (2009) Black carbon relationships with emissions and meteorology in Xi'an, China. *Atmospheric Research*, 94, 194-202.

Cao, J., X. Tie, B. Xu, Z. Zhao, C. Zhu, G. Li & S. Liu (2011) Measuring and modeling black carbon (BC) contamination in the SE Tibetan Plateau. *Journal of Atmospheric Chemistry*, 67, 45-60.

Castro, L., C. Pio, R. Harrison, D. Smith, (1999) Carbonaceous aerosol in urban and rural European atmospheres: estimation of secondary organic carbon concentrations. *Atmospheric Environment*,33, 2771-2781.

Chen, L. W. A., J. C. Chow, B. G. Doddridge, R. R. Dickerson, W. F. Ryan, P. K. Mueller (2003) Analysis of a summertime PM2.5 and haze episode in the mid-Atlantic region. *Journal of the Air & Waste Management Association*, 53, 946–956.

Chen, M., X. M. Li, Q. Yang, G. M. Zeng, Y. Zhang, D. X. Liao, J. J. Liu, J. M. Hu & L. Guo (2008) Total concentrations and speciation of heavy metals in municipal sludge from Changsha, Zhuzhou and Xiangtan in middle-south region of China. *Journal of Hazardous Materials,* 160, 324-9.

Chow, J. C., J. G. Watson, D. H. Lowenthal, L. W. Antony Chen & N. Motallebi (2011) PM2.5 source profiles for

black and organic carbon emission inventories. *Atmospheric Environment,* 45, 5407-5414.

Deng, J., T. Wang, Z. Jiang, M. Xie, R. Zhang, X. Huang & J. Zhu (2011) Characterization of visibility and its affecting factors over Nanjing, China. *Atmospheric Research,* 101, 681-691.

Geng, F., J. Hua, Z. Mu, L. Peng, X. Xu, R. Chen & H. Kan (2013) Differentiating the associations of black carbon and fine particle with daily mortality in a Chinese city. *Environment Research,* 120, 27-32.

Huang, K., G. Zhuang, Y. Lin, J. S. Fu, Q. Wang, T. Liu, R. Zhang, Y. Jiang, C. Deng, Q. Fu, N. C. Hsu & B. Cao (2012) Typical types and formation mechanisms of haze in an Eastern Asia megacity, Shanghai. *Atmospheric Chemistry and Physics,* 12, 105-124.

Hou, B., G.S. Zhuag, R. Zhang, T. N. Liu, Z. G. Guo, Y. Chen (2011) The implication of carbonaceous aerosol to the formation of haze: Revealed from the characteristics and sources of OC/EC over a mega-city in China. *Journal of Hazardous Materials,* 190, 529–536

Lan, Z.J., X, F. Huang, K.Y. Yu, T.L. Sun, L.W. Zeng & M. Hu (2013) Light absorption of black carbon aerosol and its enhancement by mixing state in an urban atmosphere in South China. *Atmospheric Environment,* 69, 118-123.

Latha, K. M. & K. V. S. Badarinath (2005) Seasonal variations of black carbon aerosols and total aerosol mass concentrations over urban environment in India. *Atmospheric Environment,* 39, 4129-4141.

Lee, K. H., Y. J. Kim & M. J. Kim (2006) Characteristics of aerosol observed during two severe haze events over Korea in June and October 2004. *Atmospheric Environment,* 40, 5146-5155.

Li, W. J., L. Y. Shao & P. R. Buseck (2010) Haze types in Beijing and the influence of agricultural biomass burning. *Atmospheric Chemistry and Physics,* 10, 8119-8130.

Lin, M. (2012) Regression Analyses between Recent Air Quality and Visibility Changes in Megacities at Four Haze Regions in China. *Aerosol and Air Quality Research*,12,1049-1061.

Lyamani, H., F. J. Olmo, I. Foyo & L. Alados-Arboledas (2008) Light scattering and absorption properties of aerosol particles in the urban environment of Granada, Spain. *Atmospheric Environment,* 42, 2630-2642.

Lyamani, H., F. J. Olmo, I. Foyo & L. Alados-Arboledas (2010) Physical and optical properties of aerosols over an urban location in Spain: seasonal and diurnal variability. *Atmospheric Chemistry and Physics,* 10, 239-254.

Lyamani, H., F. J. Olmo, I. Foyo & L. Alados-Arboledas (2011) Black carbon aerosols over an urban area in south-eastern Spain: Changes detected after the 2008 economic crisis. *Atmospheric Environment,* 45, 6423-6432.

McMeeking, G. R., N. Good, M. D. Petters, G. McFiggans & H. Coe (2011) Influences on the fraction of hydrophobic and hydrophilic black carbon in the atmosphere. *Atmospheric Chemistry and Physics,* 11, 5099-5112.

Menon, S., J.E. Hansen, L. Nazarenko, Y. Luo (2002) Climate effects of black carbon aerosols in China and India. *Science* 297, 2250-2253.

Pan, X. L., Y. Kanaya, Z. F. Wang, Y. Liu, P. Pochanart, H. Akimoto, Y. L. Sun, H. B. Dong, J. Li, H. Irie & M. Takigawa (2011) Correlation of black carbon aerosol and carbon monoxide in the high-altitude environment of Mt. Huang in Eastern China. *Atmospheric Chemistry and Physics,* 11, 9735-9747.

Park, R., D. Jacob, N. Kumar & R. Yantosca (2006) Regional visibility statistics in the United States: Natural and transboundary pollution influences, and implications for the Regional Haze Rule. *Atmospheric Environment,* 40,

5405-5423.

Pan, X. L., Z. F. Wang, X. Q. Wang, H. B. Dong, W. Zhang, A. Geaguidi, J. P. Huang (2010) Characteristics of Urban Black Carbon Concentration around 2008 Beij ing Olympic Games. *Climatic and Environmental Research*, 15, 616-623.

Qin, Y. & S. D. Xie (2012) Spatial and temporal variation of anthropogenic black carbon emissions in China for the period 1980–2009. *Atmospheric Chemistry and Physics*, 12, 4825-4841.

Quan, J., Q. Zhang, H. He, J. Liu, M. Huang & H. Jin (2011) Analysis of the formation of fog and haze in North China Plain (NCP). *Atmospheric Chemistry and Physics*, 11, 8205-8214.

Röösli, M., G. Theis, N. Künzli, J. Staehelin, P. Mathys, L. Oglesby, M. Camenzind, C. Braun-Fahrländer, (2001) Temporal and spatial variation of the chemical composition of PM10 at urban and rural sites in the Basel area, Switzerland. *Atmospheric Environment*, 35, 3701-3713.

Ram, K., M. M. Sarin & S. N. Tripathi (2012) Temporal trends in atmospheric PM(2).(5), PM(1)(0), elemental carbon, organic carbon, water-soluble organic carbon, and optical properties: impact of biomass burning emissions in the Indo-Gangetic Plain. *Environ Sci Technol*, 46, 686-95.

Ramachandran, S., T.A. Rajesh (2007) Black carbon aerosol mass densities over Ahmedabad, an urban location in western India: comparison with urban sites in Asia, Europe, Canada, and the United States. *Journal of Geophysical Research* 112, D06211.

Rehman, I. H., T. Ahmed, P. S. Praveen, A. Kar & V. Ramanathan (2011) Black carbon emissions from biomass and fossil fuels in rural India. *Atmospheric Chemistry and Physics*, 11, 7289-7299.

Schichtel, B. A., R. B. Husar, S. R. Falk, W. E. Wilson (2001) Haze trends over the United States, 1980–1995. *Atmospheric Environment*, 35, 5205–5210.

Senaratne, I., D. Shooter, (2004) Elemental composition in source identification of brown haze in Auckland, New Zealand. *Atmospheric Environment*, 38, 3049–3059.

Shores, C. A., M. E. Klapmeyer, M. E. Quadros & L. C. Marr (2012) Sources and transport of black carbon at the California–Mexico border. *Atmospheric Environment*, 70, 490-499.

Siegal, F. R. (2002) Environmental Geochemistry of Potentially Toxic Metals. Heidelberg: Springer, 7-190

Stock, M., C. Ritter, A. Herber, W. von Hoyningen-Huene, K. Baibakov, J. Gräser, T. Orgis, R. Treffeisen, N. Zinoviev, A. Makshtas & K. Dethloff (2012) Springtime Arctic aerosol: Smoke versus haze, a case study for March 2008. *Atmospheric Environment*, 52, 48-55.

Sun, D. H., J. Bloemendal, D. K. Rea (2002) Grain-size distribution function of polymodal sediments in hydraulic and aeolian environments, and numerical partitioning of the sedimentary components. *Sediment Geology*, 152, 263-277

Tiwari, S., A. K. Srivastava, D. S. Bisht, P. Parmita, M. K. Srivastava & S. D. Attri (2013) Diurnal and seasonal variations of black carbon and PM2.5 over New Delhi, India: Influence of meteorology. *Atmospheric Research*, 125-126, 50-62.

Tripathi, S. N., A. K. Srivastava, S. Dey, S. K. Satheesh & K. Krishnamoorthy (2007) The vertical profile of atmospheric heating rate of black carbon aerosols at Kanpur in northern India. *Atmospheric Environment*, 41,

6909-6915.

Wang, R., S. Tao, W. Wang, J. Liu, H. Shen, G. Shen, B. Wang, X. Liu, W. Li, Y. Huang, Y. Zhang, Y. Lu, H. Chen, Y. Chen, C. Wang, D. Zhu, X. Wang, B. Li, W. Liu & J. Ma (2012) Black Carbon Emissions in China from 1949 to 2050. *Environmental Science & Technology*, 46, 7595-7603.

Wang, Y., G. Zhuang, Y. Sun & Z. An (2006) The variation of characteristics and formation mechanisms of aerosols in dust, haze, and clear days in Beijing. *Atmospheric Environment*, 40, 6579-6591.

Weingartner, E., H. Saathoff, M. Schnaiter, N. Streit, B. Bitnar, U. Baltensperger (2003) Absorption of light by soot particles: determination of the absorption coefficient by means of aethalometers. *Aerosol Science* 34, 1445-1463.

Weller, R., A. Minikin, A. Petzold, D. Wagenbach & G. König-Langlo (2013) Characterization of long-term and seasonal variations of black carbon (BC) concentrations at Neumayer, Antarctica. *Atmospheric Chemistry and Physics*, 13, 1579-1590.

Xiao, Z.M. (2011) Estimation of the Main Factors Influencing Haze, Based on a Long-term Monitoring Campaign in Hangzhou, China. *Aerosol and Air Quality Research*, 11,873-882.

Yang, L., X. Zhou, Z. Wang, Y. Zhou, S. Cheng, P. Xu, X. Gao, W. Nie, X. Wang & W. Wang (2012) Airborne fine particulate pollution in Jinan, China: Concentrations, chemical compositions and influence on visibility impairment. *Atmospheric Environment*, 55, 506-514.

Zhao, Y., M. Hu, S. Slanina & Y. Zhang (2007) The molecular distribution of fine particulate organic matter emitted from Western-style fast food cooking. *Atmospheric Environment*, 41, 8163-8171.

Zhou, J. (2012) Carbonaceous and Ionic Components of Atmospheric Fine Particles in Beijing and Their Impact on Atmospheric Visibility. *Aerosol and Air Quality Research*, 12, 492-502.

Zhou, X. H., J. Gao, T. Wang, W. S. Wu, W. X. Wang (2009) Measurement of black carbon aerosols near two Chinese megacities and the implications for improving emission inventories. *Atmospheric Environment,43*,3918-3924.

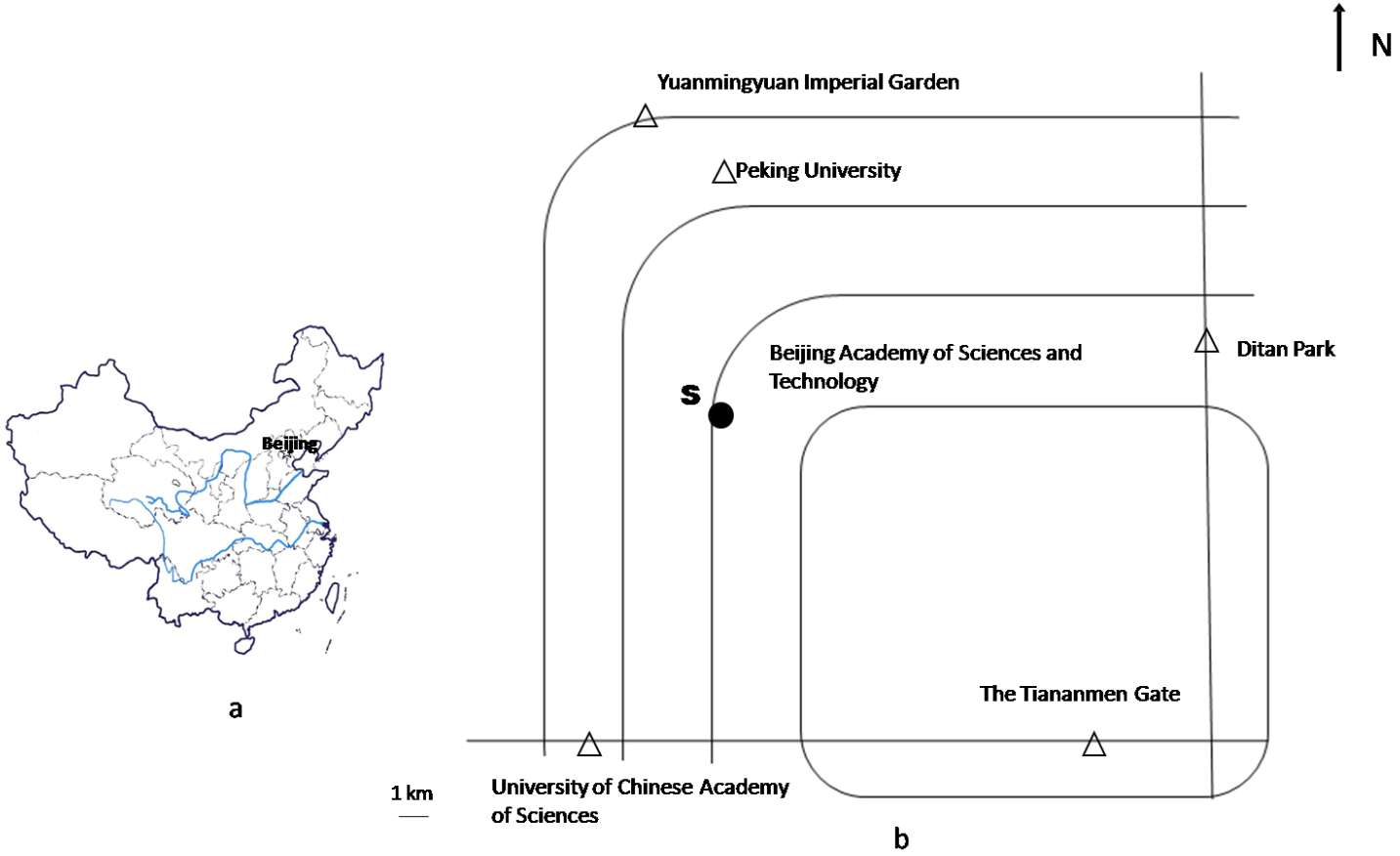

Figure 1 Sampling site location in Beijing

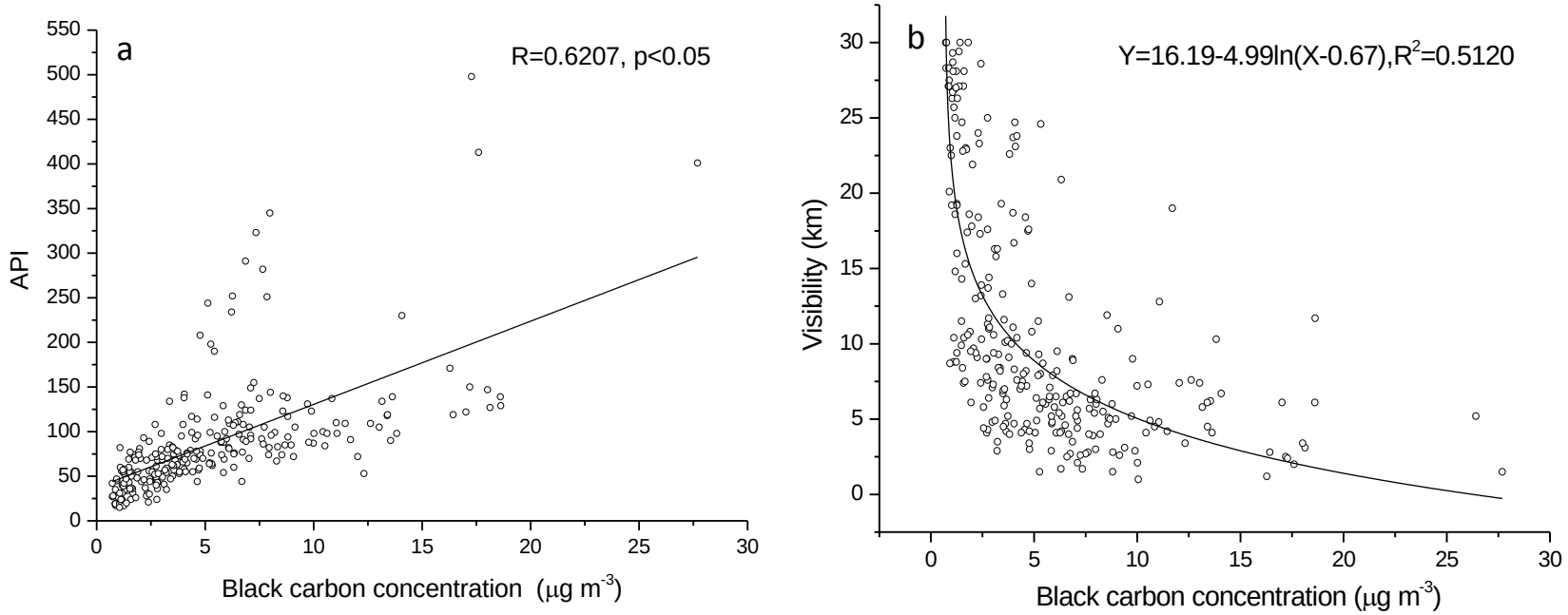

Figure 2 Relationship of black carbon concentration with API(a) and visibility(b) during the sample period in Beijing.

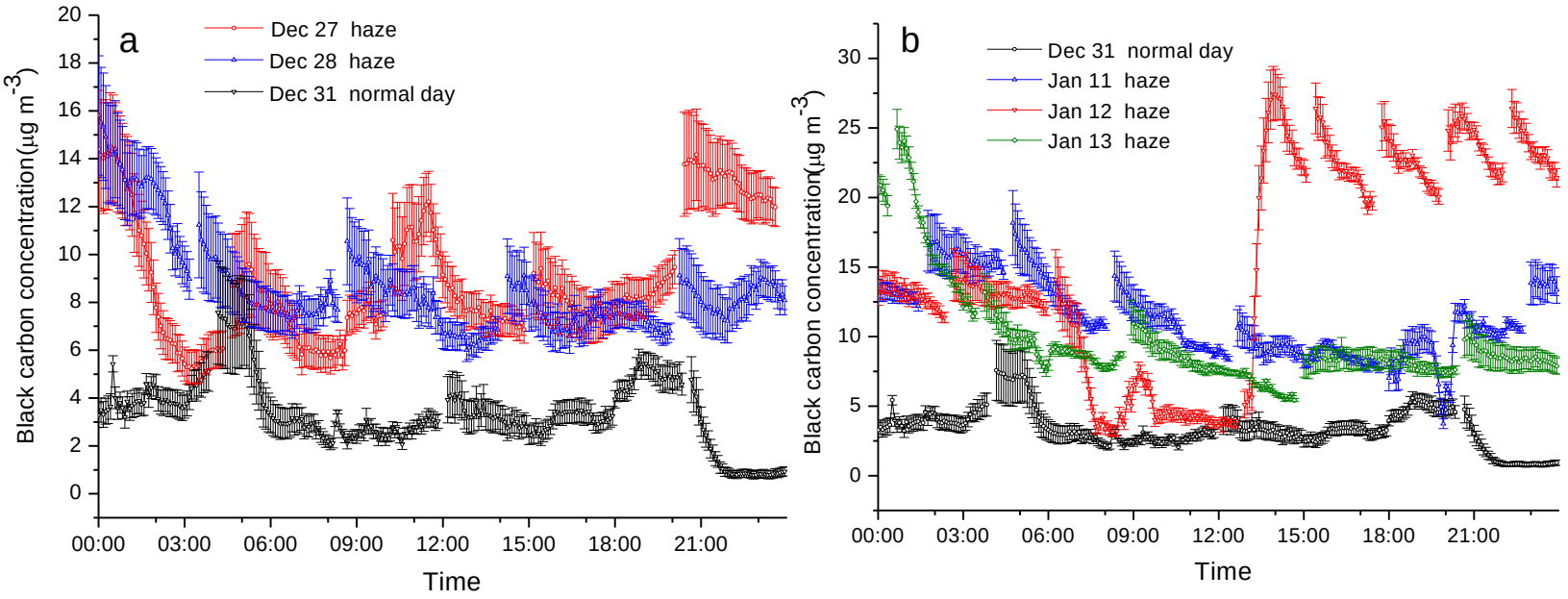

Figure 3 5-min average variations of black carbon concentration during a normal day and haze episodes.

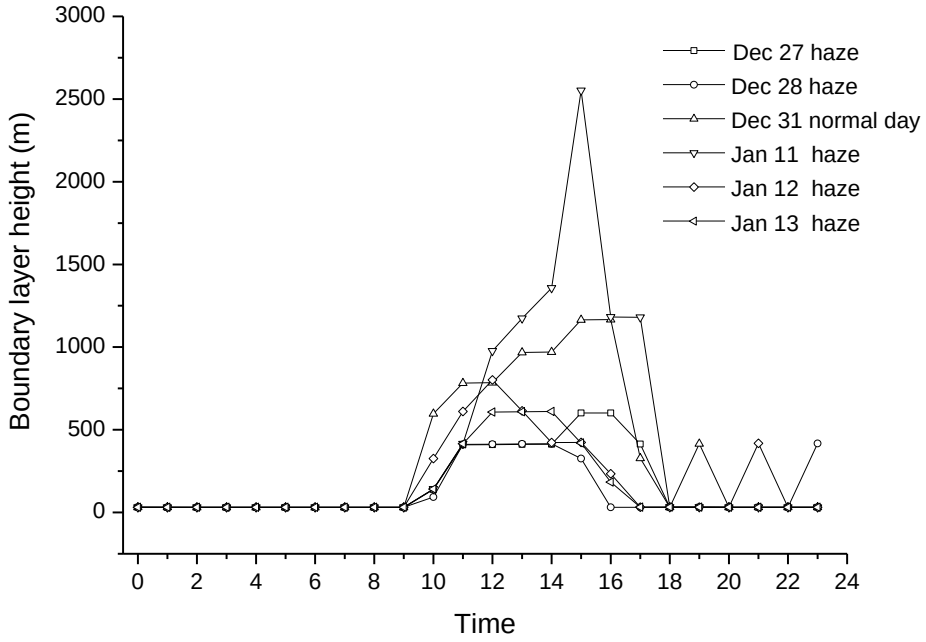

Figure 4 1-hour variations of boundary layer height during a normal day and haze episodes.

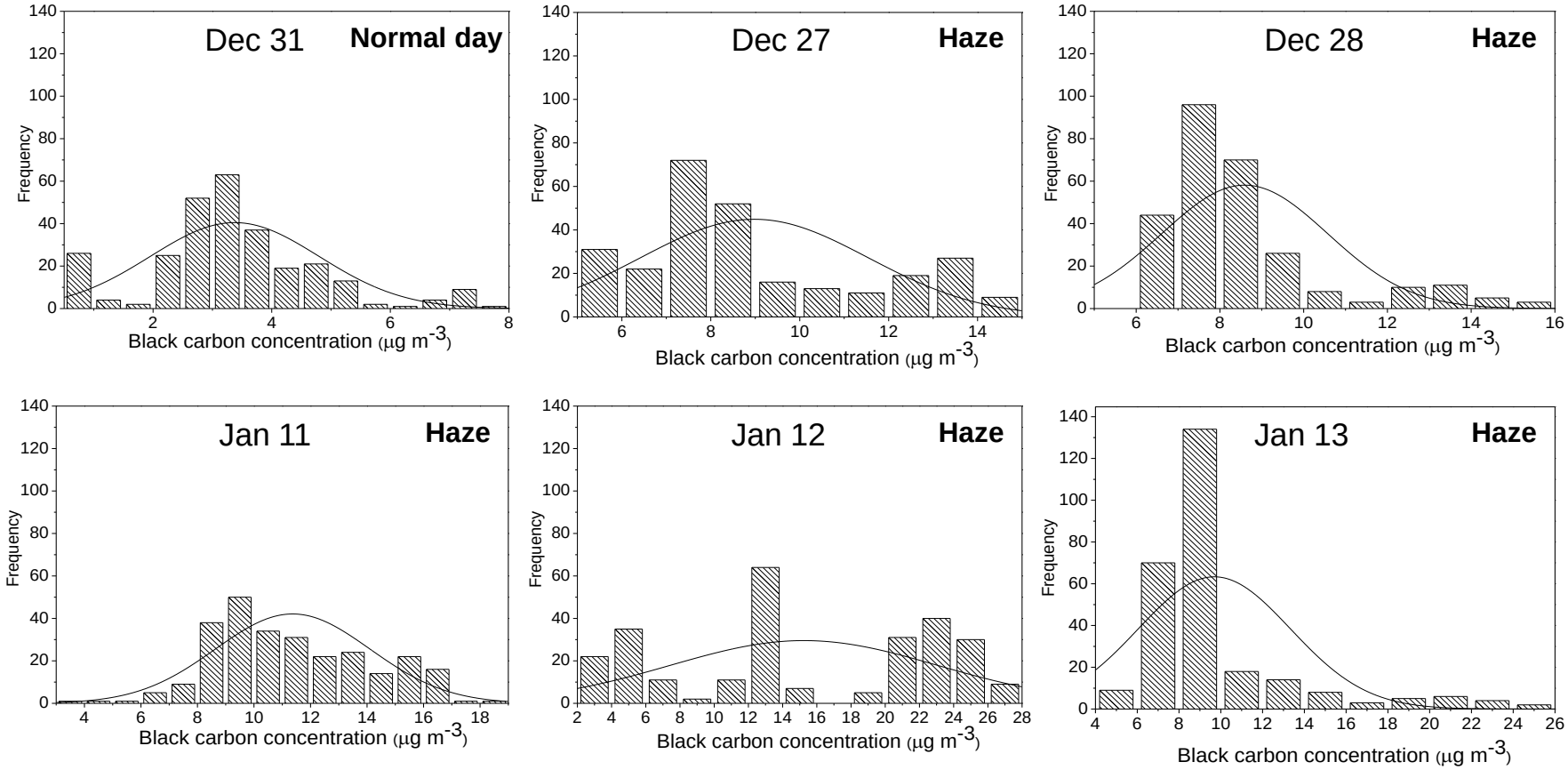

Figure 5 Frequency distribution of black carbon concentration during a normal day and haze episodes.

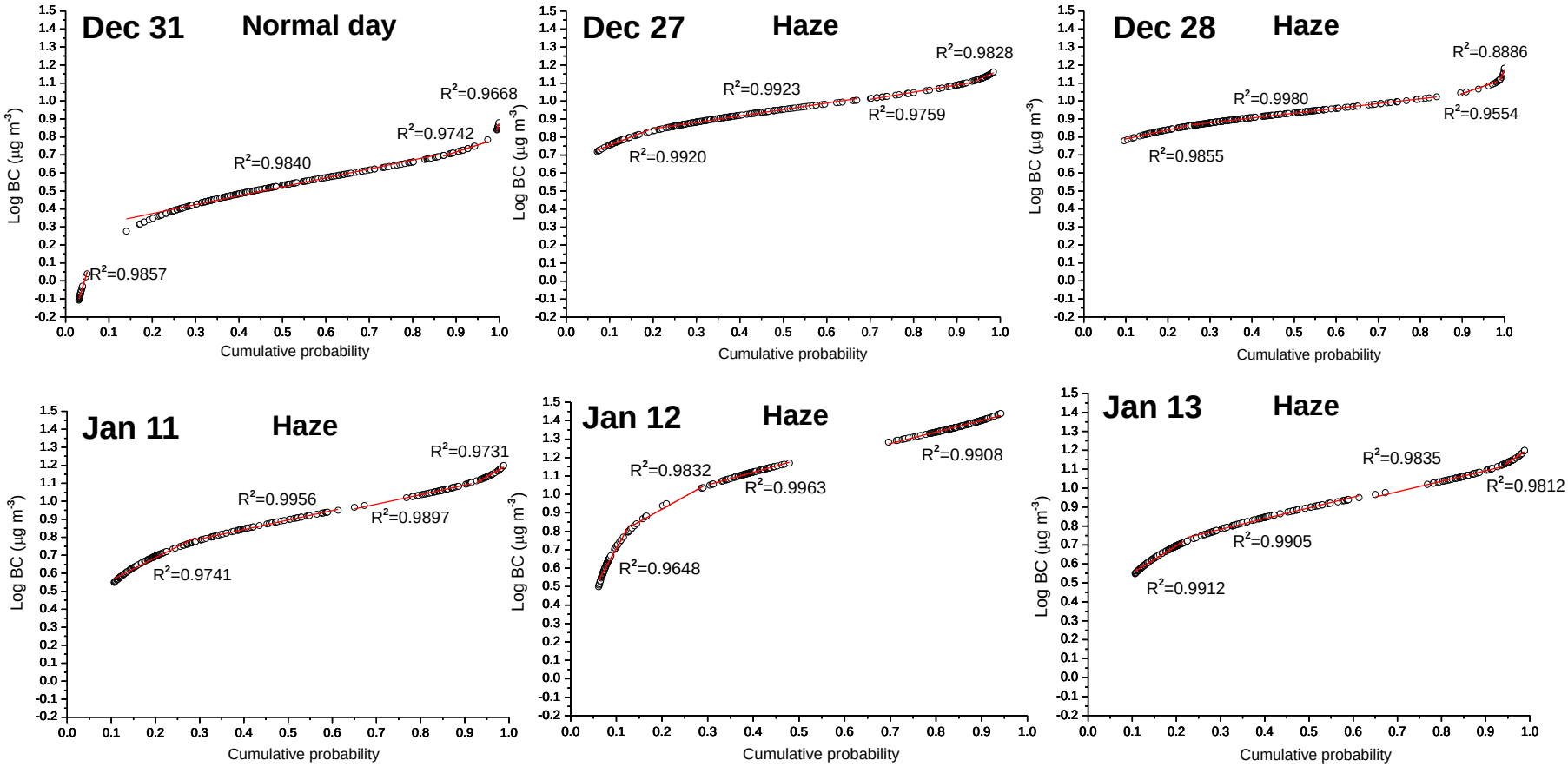

Figure 6 Plots of cumulative probability distribution versus log BC during a normal day and haze episodes.

Table 1 Statistical parameters of black carbon (μg m^{-3}) concentration and detail meteorological information per season in Beijing

Season	Average value	Standard deviation	Maximum value	Minimum value	API	RH[a] (%)	WS[b] (m/s)	Temperature （℃）	Visibility (km)
Spring	4.30	2.20	8.78	1.08	69	48	2.6	10.1	15.8
Summer	4.24	2.05	10.42	0.99	69	70	2.0	25.8	9.1
Autumn	5.97	5.14	26.41	0.73	108	60	2.3	12.3	12.7
Winter	8.14	6.37	27.69	0.92	130	73	2.0	0	3.0

[a]WS, wide speed; [b]RH, relative humidity

Table 2 Statistical parameters f black carbon (μg m^{-3}) distribution and detail meteorological information during a normal day and haze episodes.

Date	Weather	API	RH[a] (%)	WS[b] (m/s)	Temperature （℃）	Visibility (km)	Average value	Standard deviation	Variation coefficient	Skewness coefficient	Kurtosis coefficient
Dec 27	haze	119	67	1.9	-10	4.5	13.41	2.60	0.19	0.69	-0.69
Dec 28	haze	147	70	2.2	-8	3.4	18.01	2.68	0.15	1.66	2.36
Dec 31	normal	95	55	1.4	-8	10	3.91	1.40	0.36	0.55	0.94
Jan 11	haze	413	75	1.4	-4	2	17.60	2.70	0.15	0.32	-0.59
Jan 12	haze	498	81	1.1	-7	2.4	17.28	7.80	0.45	-0.13	-1.40
Jan 13	haze	401	79	1.7	-4	1.5	27.69	3.60	0.13	2.35	5.44

[a]WS, wide speed; [b]RH, relative humidity

大型环境舱协助改进外排式空气净化设备性能的评价测试

杨华，王欣欣，刘清珺，刘艳菊，邵薇
北京市理化分析测试中心，北京，100089

摘　　要： 现行空气净化器评价标准不适于外排式净化设备的性能测试。本实验通过对外排式净化设备设计、添加采样装置，在现行空气净化器评价标准基础上，以大型环境舱为检测平台，以香烟烟雾为颗粒物、甲醛、乙醛和巴豆醛等污染物的污染源，实现了净化设备的性能改进，污染物去除率从不足 5%最高升至 82.8%。

关键字：外排式空气净化设备，评价，大型环境舱，颗粒物，气体污染物

1 前言

被动吸烟对人体健康的影响已受到普遍关注[1]。环境香烟烟雾（ETS）中含有大量颗粒物及甲醛等有机污染物[2]，且其浓度远高于引起机体损伤的阈浓度[3]。香烟烟雾已成为空气净化器检测时颗粒物及气体污染物的污染源[4]。然而，现行空气净化器评价标准[4]仅对净化器的使用空间即室内进行污染物的检测，这不适于外排式净化设备（即室内污染物经抽吸净化后排向室外）的性能测试。本实验即应外排式净化设备制造者（北京中技惠民科技发展有限公司）的要求，在现行空气净化器评价标准基础上，以大型环境舱为检测平台，以香烟烟雾为颗粒物、甲醛、乙醛和巴豆醛等污染物的污染源，协助制造者对净化设备进行性能改进。

2 材料与方法

2.1 实验设备

实验用烟尘净化器为外排式室内空气净化设备(北京中技惠民科技发展有限公司提供)（见图 1），即含颗粒物及其它污染物的气体被风机（外转子轴流式风机 FZY-2E250，风量 2100 m^3/h，浙江沃尔德风机有限公司）鼓入圆柱形白铁皮反应器内，反应器内的颗粒状填料被风机鼓动成流化状态，与污染物充分混合、接触并反应，净化后的气体排出室外。受试材料为不同配比的聚苯乙烯与活性炭填料(北京中技惠民科技发展有限公司提供)，分别标记为 1#-4#。实验需根据预测试结果调整风机个数。

实验在 14 m^3 大型环境舱中进行。（HUNTER-1，北京市理化分析测试中心、中国林业科学院木材工业研究所、浙江求是人工环境有限公司）[5]。整个舱体采用不锈钢板建造，舱门开口处使用具有气密的无吸附作用的密封条进行密封。环境舱性能质量已通过“国家标准物质研究中心”计量认证。实验舱内参数设置为：温度：25℃；相对湿度：45%；空气交换率：0.25 次/小时；风速：0.1-1m/s。

在环境舱内点燃 10 支香烟（钻石牌，烤烟型，河北中烟工业有限责任公司出品），同时开启净

化器，使反应器内受试颗粒形成流化状态。10 min 后进行采样。

2.2 样品采集与分析

净化后采样：实验采用白铁皮制成圆台状采样装置。采样装置紧密固定于反应器出口处。装置顶部使用铝箔密封。顶部沿直径在圆心、距圆心 2 cm、4 cm 设三个气体采样点（见图 1）。三个采样点连接透明 PVC 软管（内径 1 cm)，三支软管经四通阀链接、混合后经环境舱采样口与舱外气体采样泵相连，经 2，4—二硝基苯肼（2，4—DNPH，分析纯）吸附管（Sep-Pack 硅胶柱，美国 Waters）吸附。使用 5 ml 乙腈注入吸附管，洗脱液定容至 5 ml 后，由液相色谱（LC-20AD，SHIMADZU，日本）进行分析。液相色谱条件：紫外检测器（工作波长 360 nm)，色谱柱 C18 反向柱；流动相比例为乙腈/水：60/40（V/V）；流速 1.0 ml/min；进样量 10 μl。

在顶部装置距圆心 3 cm 设颗粒物采样点，使用塑料管（内径 3 cm) 经环境舱采样口与舱外微电脑激光粉尘仪（LD-5C，北京绿林创新数码科技有限公司）相连，检测总悬浮颗粒物（TSP）。取采样时间 20 min 内的平均值作为检测结果。

净化前采样：在净化器进风口中心设置气体及颗粒物采样装置进行采样。样品分析同净化后样品。

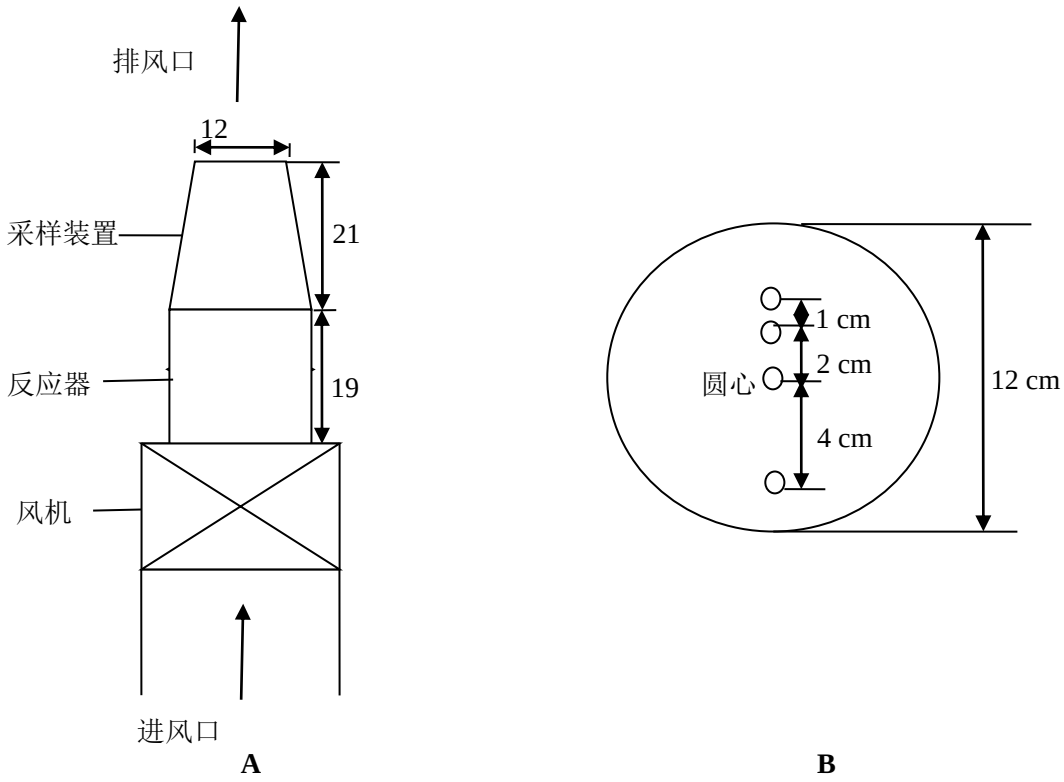

图 1 A 净化设备与采样装置简图；B 采样装置顶部采样点简图

Fig. 1 A Schematic of the cleaner and sampling unit; B Schematic of sampling points on the top of sampling unit

3 结果与讨论

本实验中，各材料对污染物的去除效果以污染物去除率表示，其定义为：

污染物去除率=（净化前污染物浓度-净化后污染物浓度）/净化前污染物浓度× D641D

预实验采用单台风机进行测试。结果显示，各污染物去除率不足 5%。通过增加至三台风机改进排风设备，测试效果较为明显。具体结果如下（图 2）：

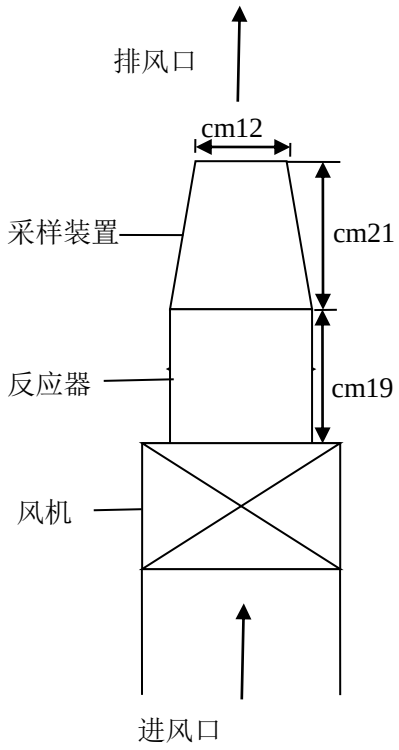

A

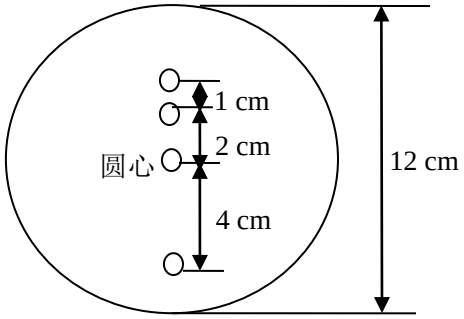

B

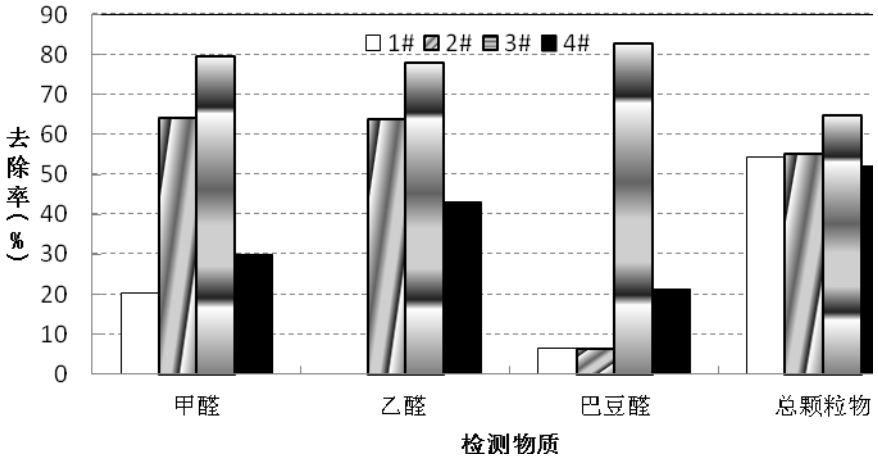

图 2 四种受试材料对污染物质的去除率

Fig. 2 Removal rates of four kinds of materials

实验结果表明，四种混合物对各污染物去除效果参差不齐，如 1#材料和 3#材料对乙醛的去除率分别为 0 和 77.8%，又如 1#材料和 3#材料对巴豆醛的去除率分别为 6.4%和 82.8%。但四种混合物对总颗粒物的去除率却差异不大，均在 52%-64.7%之间。

整体上，四种混合物对污染物的去除效果呈现优劣。3#材料对甲醛、乙醛、巴豆醛以及总颗粒物等 4 种污染物的去除率在 60%-90%之间，在四种受试材料中去除率最高，其去污性能最佳；2#材料对（除巴豆醛外）3 种污染物的去除率仅次于 3#材料，其去除率在 50%-70%之间；4#材料对污染物（除总颗粒物外）的去除率高于 1#材料，去除率在 20%-60%之间；1#材料对甲醛、乙醛、巴豆醛的去除率均低于其它三种材料，而对总颗粒物的去除率为 54.2%，该去除率高于 4#材料。

环境舱具有温湿度均匀可控，吸附性小，本底浓度低、操作便捷安全，能够较真实地模拟受污染的室内环境的特点。本实验针对原有净化设备设计、添加采样装置，尝试以环境舱为测试平台，实现了净化设备的研发改进。本实验需继续补充室内净化效果的评价测试。

致谢

本实验得到北京市科技新星计划（Z121103002512035）、国家自然科学基金项目（No. 40875082，21207007）的支持，在此表示感谢。

参考文献

[1] 甘德坤，焦力，朴文花，马玲，何兴舟. 环境香烟烟雾对非吸烟人群健康影响研究进展. 环境与健康杂志，2000，17（2）：125-128

[2] 郑聪. 环境烟草引起的室内空气污染的定量研究[硕士学位论文]. 湖南大学，2007

[3] 杨湘山，赵淑华，吕焱，刘洪阳，赵力，李景舜. 香烟烟雾中 SO_2、NO_X 和甲醛浓度的测定及评价，安全与环境学报，2005，5（3）：45-46

[4] 中华人民共和国国家质量监督检验检疫局，中国国家标准化管理委员会. GB/T 18801-2008 空气净化器，中国标准

出版社出版发行，2009. 1-19

[5] 杨华，赵明明，刘艳菊.大型环境舱单舱检测被动式空气净化产品. 上海师范大学学报（自然科学版），2011，40（6）：600-603